



Deliverable D4.3.2 – Innovative Concepts for Bottom-Mounted Structures

Partners WP4 Task 4.3
OLD, DTU, LUH, RAW

September, 2014

Agreement n.:	308974
Duration	November 2012 – October 2017
Co-ordinator:	Danmarks Tekniske Universitet
Supported by:	FP7 – EU Programme



The research leading to these results has received funding from the European Community's Seventh Framework Programme FP7-ENERGY-2012-1-2STAGE under grant agreement No. 308974 (INN WIND.EU).

PROPRIETARY RIGHTS STATEMENT

This document contains information, which is proprietary to the "INN WIND.EU" Consortium. Neither this document nor the information contained herein shall be used, duplicated or communicated by any means to any third party, in whole or in parts, except with prior written consent of the "INN WIND.EU" consortium.

Document information

Document Name:	Deliverable D4.3.2. – Innovative Concepts for Bottom-Mounted Structures
Confidentiality Class	Public
Document Number:	Deliverable D 4.3.2
Author:	OLD: Bernd Kuhnle DTU: Mathias Stolpe , Anand Natarajan, Tomas Hanis LUH: Jan Häfele Ramboll: Thomas von Borstel
Review:	Ramboll: Tim Fischer
Date:	2014-09-19
WP:	4 Offshore Foundations and Support Structures
Task:	4.3 Structural Implementation

Table of Contents

1	INTRODUCTION.....	3
2	DESIGN ASSUMPTIONS.....	5
3	STRUCTURAL CONCEPTS	6
3.1	Truss-towers and jacket-variants.....	6
3.1.a	Objectives and design methodology	6
3.1.b	Analysis model, parameters, and implementation.....	7
3.1.c	Design concepts.....	8
3.1.d	Jackets with three legs.....	8
3.1.e	A full-lattice tower with three legs and 10 levels of X-braces	10
3.1.f	Design results.....	11
	References.....	15
3.2	Smart jacket.....	16
3.2.a	Design concept.....	16
3.2.b	Design results.....	20
3.2.c	Conceptual conclusions and outlook	25
3.3	Hybrid jacket	26
3.3.a	Introduction	26
3.3.b	Design process.....	29
3.3.c	Conclusion and Outlook.....	35
	References.....	35
3.4	Jacket-Bucket-Concept.....	36
3.4.a	Introduction	36
3.4.b	Design of Suction Buckets for the Reference Jacket	38
3.4.c	Conclusion and Outlook.....	46
	References.....	47
4	CONCLUSIONS AND OUTLOOK	49

1 INTRODUCTION

The scope of the INNWIND.EU is on high performance innovative design of a beyond-state-of-the-art 10-20MW offshore wind turbine. Within this framework, different parts of the wind turbine are scrutinized. WP4 is therefore focussing on innovations on component level for the support structure and their design implementation in innovative support structures. To widen the view and not been limited on one support structure solutions, this report shall investigate innovative support structure concepts, their influence on the overall design and their potential for cost savings.

Four partners contributed to this deliverable D4.32: “Innovative Concepts for Bottom-Mounted Structures”, namely the Danish Technical University (DTU), ForWind – Oldenburg, Leibniz University of Hanover and Rambøll.

These four partners present four different concepts which are:

- Truss towers and Jacket variants
- Smart jacket
- Hybrid jacket
- Jacket-Bucket-Concept

These concepts are, however, in completely different development stages. Whereas jacket variants are already rarely used and installed and damping devices are already applied, the concept of suction bucket foundations for offshore wind turbines had recently its first installation and the hybrid jackets are not yet used.

All partners give an in-depth insight in the design methodologies and describe issues and limitations in the process. They identify the potential of their innovative concept under use of simulations or analytical approaches and compare it to the reference jacket in terms of material needed, designing loads and/or installation obstacles.

DTU presents three different concepts. The first and second concepts are three legged jackets with a different number of levels. The third concept is a full-lattice tower with three legs. Structural optimizations are performed with the goals of mass reduction and reduction of the first natural frequency of the system. Another target is the reduction of welded connections which are also one of the cost drivers for offshore support structures.

ForWind – University of Oldenburg carried out simulation to evaluate the effect integrated tuned mass dampers in the INNWIND.EU reference turbine. Parameter studies, varying e.g. the damper mass ratio and tuning frequency, are therefore performed to proof the concept in aero-elastic simulations.

Leibniz University of Hanover investigates the effect of substituting steel members by hybrid members. Especially the resulting change in natural frequency, which is an important driver for the support structure fatigue and therefore lifetime of the jacket, is in the focus of the assessment.

Rambøll applies standard design methodologies for suction bucket foundations to proof this concept for a four-legged jacket for the INNWIND.EU reference turbine.

Section 2 firstly gives a short overview over principle assumptions the partners made. In section 3, the concept evaluations and conclusions by the partners are found. Section 4 finally tries to conclude the partners’ contributions.

2 DESIGN ASSUMPTIONS

Design assumptions are important to assess the important aspects of the individual innovative concepts and to be able to discuss the outcomes. Each partner defined them individually, however some assumption are common for all partners. They are summarized in the following.

DTU refers to the common INNWIND.EU reference design [01, 02, 03]. However, during the design optimization, fatigue loads were neglected and only extreme loads and static loading were taken into account. The influence of the soil on the support structure, which was already assessed in [04], as well as safety factors were also neglected.

ForWind – Oldenburg also used the INNWIND.EU reference design [01, 02, 03] as starting point. Fatigue loads were in the focus of the investigations and extreme loads were neglected. Only power production cases were taken into account and no safety factors were applied in the simulations.

Leibniz University of Hannover also referred to the INNWIND.EU reference design [01, 02, 03]. Taking the basic geometric parameters into account, variations of the member parameters, such as the ratio of steel to sandwich material, were investigated and the effect on natural frequencies compared to the reference structure was evaluated.

Rambøll's work is also based on the INNWIND.EU reference design. However, no cyclic loading was taken into account in the design process for the suction buckets. Anyhow, soil parameters and safety factors are considered and the design process is adapted to the standard design process for suction bucket foundation.

[01] T. v. Borstel, "INNWIND.EU Deliverable 4.3.1 Design Report Reference Jacket," INNWIND.EU, 2013.

[02] "INNWIND.EU – 10MW Jacket Interface Document for Preliminary Jacket Design," INNWIND.EU, 2013.

[03] "INNWIND.EU Deliverable 1.2.1 Definition of Reference Wind Turbine," INNWIND.EU, 2013.

[04] INNWIND.EU Deliverable D4.12., "Innovations on component level", 2014

3 STRUCTURAL CONCEPTS

3.1 Truss-towers and jacket-variants

Mathias Stolpe (matst@dtu.dk), Anand Natarajan (anat@dtu.dk), and Tomas Hanis (tohani@dtu.dk)

3.1.a Objectives and design methodology

The main objective is to present alternative bottom-fixed support structural concepts for the INN WIND.EU 10 MW reference turbine described in [DTU01]. The concepts are alternatives to the **preliminary** four legged reference jacket presented in [DTU02]. Three design concepts are proposed. The first and second concept are jackets with three legs which are coupled to the reference tower described in [DTU03] with one concept having three levels of X-braces and another with four levels of X-braces. The third design concept is a full-lattice tower with three legs.

The preliminary design, i.e. the choice of overall dimensions and member sizing, of these three different topologies has been done entirely using techniques from structural optimization. The objective function in all optimization processes has been the structural mass throughout in an attempt to reduce the material cost of the structures (for the given topology). For the optimization process static estimates of extreme tower top loads [ref] have been used. The constraints include limits on the overall structural bending stiffness, local ultimate strength in the members, and fundamental eigenfrequencies. The requirements have been to reduce the first fundamental eigenfrequency compared to the four legged preliminary reference jacket in an attempt to reduce fatigue loads. For some of the suggested structures higher frequencies have been reduced. In particular, the first torsion mode has been reduced compared to the four legged jacket from [DTU02] since it allowed further reductions of the first eigenfrequencies. Soil structure interaction is neglected and the soil connectivity is considered to be rigid and fixed.

The simultaneous overall dimensioning and preliminary optimal design of jacket sub-structures for offshore wind turbines has been done using structural optimization. The basic topology, i.e. the connectivity of the structure is assumed to be fixed and the initial concept is depicted in Figure 3.1-1. The structural dimensions are described by two types of design variables. The outer variables model overall dimensions of the structure, such as the base and top widths, and the transition jacket height. The outer variables also model the locations of the X- and K-joints in the classical jacket structures, see Figure 3.1-2. The inner design variables represent the dimensions of the members in the ground structure representing the jacket structure, i.e. the inner diameters and the thickness distribution of the members that constitute the X-braces, mud-braces, legs etc. The structural optimization also contains dimensioning of a simple space frame (called the transition jacket) which connects the jacket to the tower, see Figure 3.1-1 and Figure 3.1-2. For the full-lattice jacket the original tower is replaced by a very short beam.

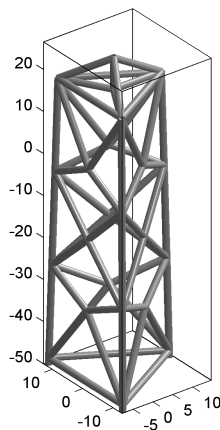


Figure 3.1-1: Basic topology (connectivity) before optimization for a jacket with three legs and three levels of X-braces. The figure also shows the connectivity chosen for the transition jacket.

Besides the mechanical constraints on strength, stiffness and eigenfrequencies a number of geometric couplings are included (through constraints in the inner and outer optimization problems) on the structure. The members of an X-brace for a specific level in the structure are all constrained to have the same thickness and diameter. Likewise, the leg members in a specific section also have the same dimensions. Additionally, some amount of symmetry is also enforced on the final structure. The legs are furthermore forced to be straight and the positions of the K-joints are only allowed to move along the length of the legs. Similarly, the positions of the X-braces are constrained to be in the middle of the planes spanned by the relevant legs. There are also constraints on the diameter over thickness ratio.

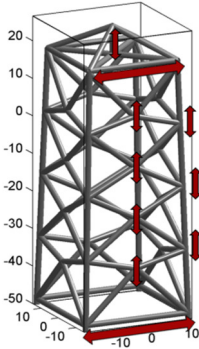


Figure 3.1-2: Definition of the outer design variables used for overall dimensioning of a given topology. Here the variables are exemplified on a jacket with four legs and four levels of X-braces.

The conceptual decisions on number of legs or number of levels of X-braces are not included in the optimization problem. They are instead taken care of by parametric studies. The (realistic) number of combinations of legs and X-braces is fairly modest and enumeration is possible. The design of the sub structures was made to save material cost and also reduce the number of welded connections as far as possible, but with constraints on member dimensions so that the von Mises stress failure criteria is not violated at any member. The resulting jacket designs can serve as the starting point for detailed design of the individual members with fatigue damage assessments and soil pile interactions.

3.1.b Analysis model, parameters, and implementation

The structural response is computed by the finite element method for linear elasticity. The code uses tubular beam elements based on Timoschenko beam theory for the legs, braces, and tower. The code, which is called JacketOpt, is developed and implemented at DTU Wind Energy. It is specifically designed to efficiently compute both relevant functions (displacements, stresses, eigenfrequencies, etc.) and their derivatives with respect to the design variables.

The extreme thrust force at tower top (located at 115.63 m) is set to 4800 kN with a simultaneous bending moment of 18000 kNm [DTU03]. Both quantities include partial safety factor for the loads. A concentrated vertical load from the tower top mass is also included in the model. These loads are assumed to be independent of all design variables. The hydrodynamic forces on the jacket structure are computed using Morison's equation. From a wave simulation time series, a single time step is chosen as a static representative of the wave loads at the point of peak inertial loading.

For all structures top displacement constraints are included to model overall structural stiffness. The tower top is not allowed to move more than 2.25 m in any direction under the above mentioned extreme loads. The von Mises stresses are not allowed to exceed 355 MPa anywhere in the jacket sub-structure. The stresses are measured at the end nodes of the finite elements at eight different positions evenly spaced around the tubular cross-sections. The material safety factor for the strength constraints is set to 1.15.

The dimensions of the tower are not included in the optimization process, although the code has this capability. This decision was made since we would like to be able to compare the results with the four legged jacket proposed in [DTU02] and the reference tower from

[DTU03]. The model of the tower used in the numerical experiments closely follows the model of the reference tower presented in [DTU03]. The tower is partitioned into ten prismatic segments with circular cross-sections each with constant thickness and diameter. This is in contrast to the reference tower which consists of conical segments. The tower mass in the model is 474.3 tonnes.

The rotor-nacelle assembly is modeled as a lumped mass of 676,723 kg at the tower top (at height 115.63 m) together with a moment of inertia about the x-axis of $1.66 \cdot 10^8 \text{ kg m}^2$, a moment of inertia about the y-axis of $1.27 \cdot 10^8 \text{ kg m}^2$, and a moment of inertia about the z-axis of $1.27 \cdot 10^8 \text{ kg m}^2$ [DTU01]. The Young's modulus and density for steel are throughout assumed to be 210 GPa, and 7850 kg/m³ for the jacket structures. For the tower the density is adjusted following [DTU03] to 8500 kg/m³ to account for the mass of secondary structures.

Marine growth has not been included in the numerical experiments. Secondary structures such as boat landings, J-tubes, sacrifice anodes, ladders, etc. are not included in the models. The jacket structures are assumed to be fully clamped at the sea bed, hence no modeling of the soil-foundation is taken into account.

The outer optimal design problem, i.e. overall dimensioning, is solved by a derivative free optimization method, see e.g. [DTU04], since analytical sensitivities for the considered type of variables are difficult to derive and they are also expensive to estimate using finite differences. Furthermore, the outer problem has a rather small number of variables and only linear constraints. It is thus a good candidate for derivative free methods. The inner problem formulations, i.e. member sizing, are solved using a robust efficient modern derivative based optimization methods based on Sequential Quadratic Programming (SQP), see e.g. [DTU05]. The optimization process was given 48 computation hours on a single core of an Intel Xeon X5650 6-core CPUs, running at 2.66 GHz and with 4 GB Memory for each core.

3.1.c Design concepts

Three different design concepts obtained by structural optimization are presented below. The first is a three legged jacket with three levels of X-braces. The second is a three legged jacket with four levels of X-braces. The third design concept is a three legged full lattice tower with 10 levels of X-braces.

3.1.d Jackets with three legs

For the design of a jacket with three legs we have chosen to use both three and four levels of X-braces. For these jackets the first and second eigenfrequency are constrained to be in the interval [0.24, 0.27] Hz so that it is less than 3P, while the third frequency is forced inside the interval [0.52, 0.58] Hz, i.e. in between the 3P and 6P frequency intervals for the 10 MW reference turbine [DTU03]. The higher frequencies are forced to be above 1 Hz. The lower and upper bounds on the outer design variables are listed in Table 3.1-1 for the jackets with three legs while the bounds on the inner design variables are listed in Table 3.1-2.

Table 3.1-1: Bounds on the outer design variables for the jackets with three legs.

Description	Lower bound [m]	Upper bound [m]
Half base width	8	18
Half top width	6	12
Transition jacket height	5	10

Table 3.1-2: Bounds on the inner design variables for the jackets with three legs.

Description	Lower bound [mm]	Upper bound [mm]
Legs wall thickness	20	120
Braces etc. wall thickness	10	120
Legs inner radius	250	2000
Braces etc. inner radius	150	1000

The jackets obtained as a result of the structural optimization process are shown in Figure 3.1-11 and Figure 3.1-12. The first five fundamental frequencies for these structures are listed in Table 3.1-3 and Table 3.1-4. The main characteristics of the jackets are listed in Table 3.1-5.

Table 3.1-3: The first five natural frequencies for the entire system for the three legged jacket with three levels of X-braces shown in Figure 3.1-11. The analysis is performed in ABAQUS using Timoschenko beam elements.

Mode/ Frequency [Hz]	1 st Bending	1 st Bending	Torsion	2 nd Bending	2 nd Bending
	0.262	0.263	0.574	1.129	1.171

Table 3.1-4: The first five natural frequencies for the entire system for the three legged jacket with four levels of X-braces shown in Figure 3.1-12. The analysis is performed in ABAQUS using Timoschenko beam elements.

Mode/ Frequency [Hz]	1 st Bending	1 st Bending	Torsion	2 nd Bending	2 nd Bending
	0.261	0.263	0.575	1.125	1.167

Table 3.1-5: Overview of the geometry and masses of the three legged jackets.

Description	Unit	Three X-brace levels	Four X-brace levels
Half base width	[m]	18	18
Half top width	[m]	11.9	11.9
Transition jacket height	[m]	10	10
Jacket legs inner radius	[mm]	0.594	0.603
Jacket legs max wall thickness	[mm]	45	43
Jacket legs min wall thickness	[mm]	35	34
Total jacket mass	[tonnes]	530.2	539.8
Jacket mass (excl. transition)	[tonnes]	272.9	281.5
Transition jacket mass	[tonnes]	257.3	258.3
Total legs mass	[tonnes]	220.3	218.9
Total X-braces mass	[tonnes]	52.7	62.5

For the jackets with three legs the dimensions of all X-braces and the mud-braces are all at the lower bounds, i.e. the thickness is 10 mm and the inner radius is 150 mm. The dimensions have in this case not been chosen because of the mechanical requirements but rather on the geometric constraints and the choice of objective function. This indicates that

the simplified loads and the chosen constraints (and constraint limits) are not governing their design and detailed full load analysis from aeroelastic simulations may be necessary.

3.1.e A full-lattice tower with three legs and 10 levels of X-braces

For the design of a full-lattice tower with three legs we have chosen to use ten levels of X-braces. The bounds on the inner and outer design variables for this structure are listed in Table 3.1-6 and Table 3.1-7, respectively. For the full lattice tower the lower three eigenfrequency are constrained to be in the interval [0.24, 0.265] Hz. while the higher frequencies are forced to be above 1 Hz.

Table 3.1-6: Bounds on the outer design variables for the full-lattice tower.

Description	Lower bound [m]	Upper bound [m]
Half base width	8	12
Half top width	4	8
Transition jacket height	3	6

Table 3.1-7: Bounds on the inner design variables for the full-lattice tower.

Description	Lower bound [mm]	Upper bound [mm]
Legs wall thickness	20	120
Braces etc. wall thickness	10	120
Legs inner radius	250	2000
Braces etc. inner radius	150	1000

Table 3.1-8: The first five natural frequencies for the entire system for the three legged full-lattice tower with ten levels of X-braces shown in Figure 3.1-10. Note that the lowest frequency corresponds to the first torsion mode. The analysis is performed in ABAQUS using Timoschenko beam elements.

Mode/ Frequency [Hz]	1 st Bending	1 st Bending	Torsion	2 nd Bending	2 nd Bending
	0.264	0.265	0.254	1.260	1.390

The full-lattice tower obtained by structural optimization is shown in Figure 3.1-10 and the main characteristics are listed in Table 3.1-9. The first five fundamental frequencies for this structure are listed in Table 3.1-8.

Table 3.1-9: Overview of the geometry and masses of the full-lattice tower.

Description	Unit	Ten X-brace levels
Half base width	[m]	10.7
Half top width	[m]	6.3
Transition jacket height	[m]	4.97
Jacket legs inner radius	[mm]	0.611
Jacket legs max wall thickness	[mm]	61
Jacket legs min wall thickness	[mm]	20
Total jacket mass	[tonnes]	736.9
Jacket mass (excl. transition)	[tonnes]	641.5
Transition jacket mass	[tonnes]	95.4
Total legs mass	[tonnes]	538.4
Total X-braces mass	[tonnes]	103.1

For the full-lattice jacket with three legs, the dimensions of all X-braces and the mud-braces are almost all at the lower bounds, i.e. the thickness is 10 mm and the inner radius is 150 mm. The top and bottom X-braces have slightly larger inner diameters. The dimensions have in this case (again) not been chosen because of the mechanical requirements but rather on the geometric constraints and the choice of objective function.

The mass for the full-lattice jacket is clearly less than the total mass of the three legged jackets with reference tower and this indicates possibilities for cost reductions, but the added cost of welding needs to be assessed. The number of X- and K-joints may substantially increase the manufacturing time and cost in comparison with reference jacket with tubular tower. However since the full lattice design is also with three legs, it presents a better solution than a four legged full-lattice tower.

The designed structures are feasible results with substantial weight savings, but have not been proven to be the optimal solution.

3.1.f Design results

The results from the structural optimization process show that it is possible to lower fundamental frequencies for these design concepts compared to the four legged jackets in both [DTU02] and [DTU01] while satisfying certain basic requirements on structural stiffness and strength. The results indicate that for the three legged jackets the mass is essentially identical for the two concepts. Since the jacket with only three levels of X-braces is less complicated it is also likely to be less expensive even after re-design for fatigue.

Figure 3.1-3 – Figure 3.1-5 show electric power curves for the three design concepts coupled to the reference tower and the INN WIND 10 MW reference turbine. The wind speed was increased linearly from 5 m/s to 25 m/s over 1900 s. The power curves were simulated using the aeroelastic software HAWC2 [DTU06]. All three curves behave as expected.

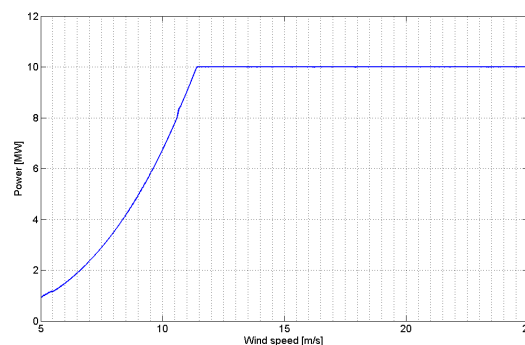


Figure 3.1-3: Power curve for the three legged jacket with three levels of X-braces.

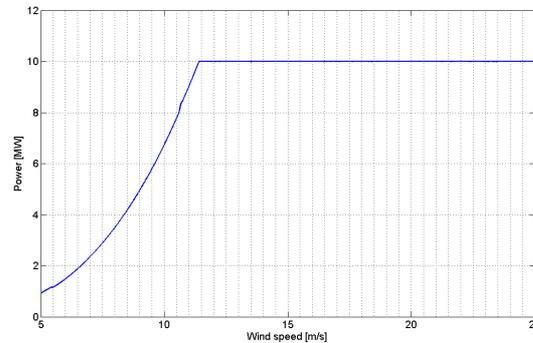


Figure 3.1-4: Power curve for the three legged jacket with four levels of X-braces.

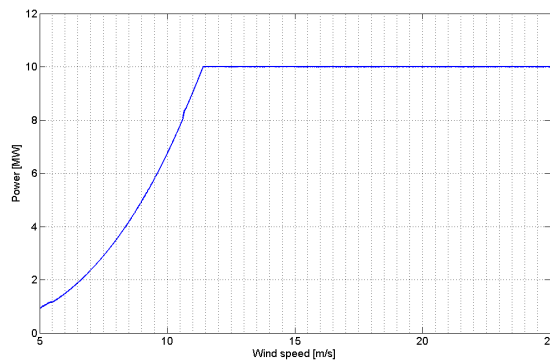


Figure 3.1-5: Power curve for the full lattice jacket.

Since fatigue and dynamic loads were not included in the structural optimization process the three described design concepts have all been coupled to the reference tower and the INN WIND 10 MW reference turbine and simulated using the aeroelastic software HAWC2. DLC 1.2 loads were simulated at 11 wind speeds (5,7,9,11,13,15,17,19,21,23,25 m/s) without yaw errors. Six seeds were used per scenario. The results are unfortunately (but not unexpectedly) rather disappointing. The stress range computations obtained by rain flow counting and the Palmgren-Miner rule at the end nodes of all the members of the three legged jacket with three levels of X-braces is shown in Figure 3.1-6. The stress range computations at the end nodes of all the members of the three legged jacket with four levels of X-braces is shown in Figure 3.1-7 and for the full lattice jacket in Figure 3.1-8. In these computations no SCFs have been used and the results should be considered as indications only. Comparing with the S-N curve from the DNV Recommended Practice [DTU07] for tubular joints in air and seawater the stress range should be below 50 MPa for 10^7 cycles. These figures indicate that there are several locations in each jacket which should be studied in more detail and redesigned.

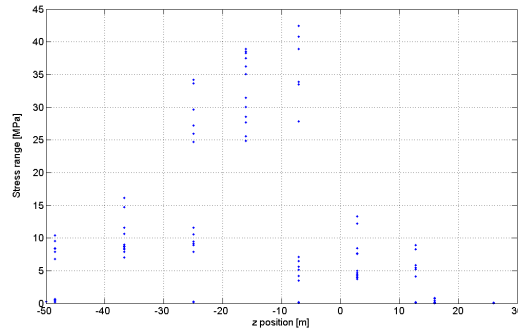


Figure 3.1-6: Indications of fatigue issues in the three legged jacket with three levels of X-braces.

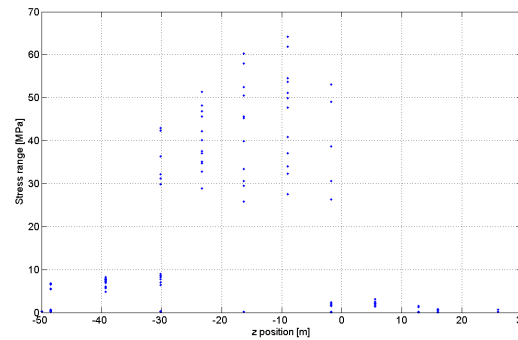


Figure 3.1-7: Indications of fatigue issues in the three legged jacket with four levels of X-braces.

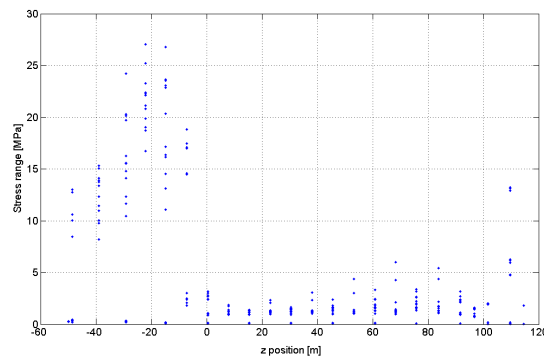


Figure 3.1-8: Indications of fatigue issues in the full lattice jacket.

For the static extreme loads used in the optimization process the limit on the von Mises stress is set to 355 MPa with a material safety factor of 1.15. An ABAQUS simulation of the extreme wind load excluding the static approximation of the wave load indicates that the limit is met in the transition jackets and parts of the legs for all design concepts see Figure 3.1-9.

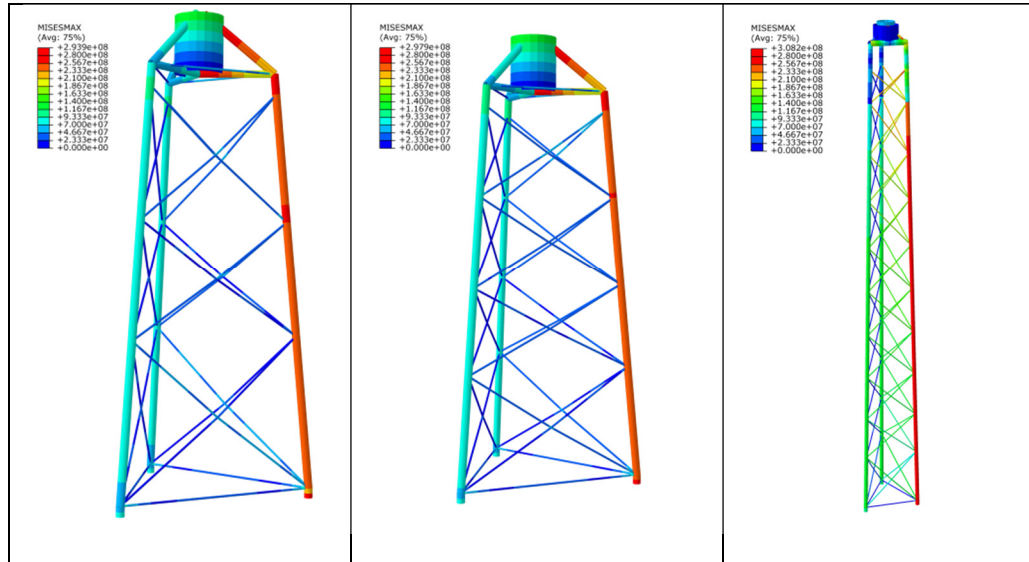


Figure 3.1-9: Stress distribution for the extreme thrust load.

Limitations to the design methodology

The perhaps most critical limitation in the structural optimization process is that dynamic loads are not included. This immediately implies that fatigue considerations are not included. The preliminary fatigue simulations indicate that resulting structures thus have a very short life time. This should (and will) be the main focus area for the detailed design phase.

Other limitations include that secondary structures are not included in the models and that no modeling of the soil-foundation interaction is taken into account.

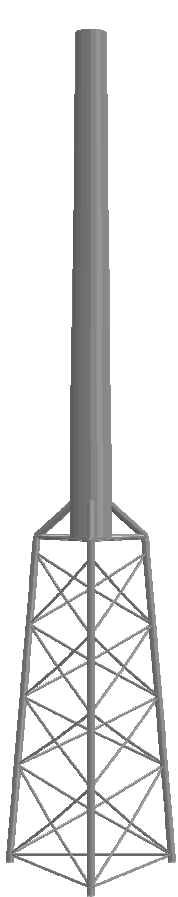


Figure 3.1-12: A jacket with three legs and four levels of X-braces.

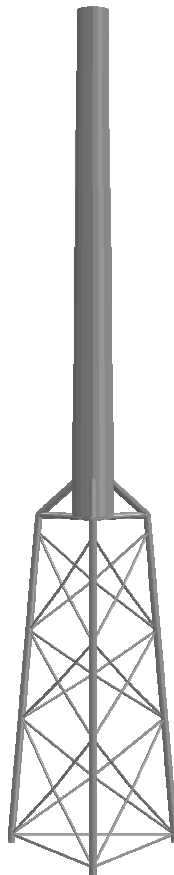


Figure 3.1-11: A jacket with three legs and three levels of X-braces obtained by structural optimization.



Figure 3.1-10: A full-lattice tower with three legs obtained by structural optimization.

References

- [DTU01] T. v. Borstel, "INN WIND.EU Deliverable 4.3.1 Design Report Reference Jacket," INN WIND.EU, 2013.
- [DTU02] "INN WIND.EU – 10MW Jacket Interface Document for Preliminary Jacket Design," INN WIND.EU, 2013.
- [DTU03] "INN WIND.EU Deliverable 1.2.1 Definition of Reference Wind Turbine," INN WIND.EU, 2013.
- [DTU04] A. R. Conn, K. Scheinberg and L. N. Vicente, "Introduction to Derivative-Free Optimization", SIAM, 2008.
- [DTU05] P. T. Boggs and J. W. Tolle, "Sequential Quadratic Programming," *Acta Numerica*, 1995.
- [DTU06] T. Larsen and A. Hansen, "How to HAWC2, the user's manual," Technical University of Denmark, 2012.
- [DTU07] DNV, "DNV-RP C203: 2012-10 DNV Recommended Practice – Fatigue Design of Offshore Steel Constructions," DNV, 2012.

3.2 Smart jacket

3.2.a Design concept

Deliverable D4.12 [ForWind-OL01] presented the design loads of the reference turbine under use of the old and the updated reference control. The second approach was an improvement in such a way that the control parameters, such as the torque gain and therefore the torque over rotor speed and/or wind speed characteristics were adjusted to match the dynamic characteristics of the reference turbine more adequately.

To understand why another iteration in the control design was necessary, the dynamics of the systems are again shown in the following. As can be seen in the Campbell diagram in figure 3.2-1, the initial rotor speed range, indicated in yellow, led to strong resonances of tower and blades with the 3P and 6P excitation in the lowest rotor speed region. As expected, the fatigue loads were highly increased and led a decreased lifetime, far below the desired design lifetime.

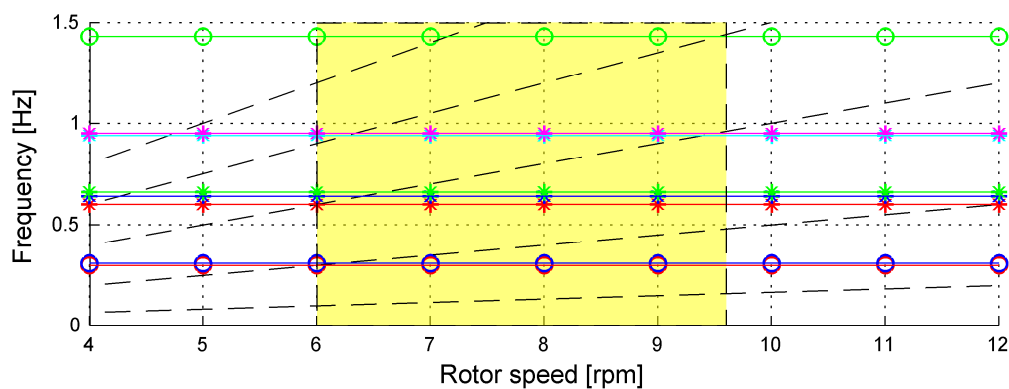


Figure 3.2-1: Campbell diagram for the INN WIND.EU reference turbine and support structure including coupled tower (circles) and blade (star) modes - operational region indicated by the yellow box [ForWind-OL01]

The lower rotational speed limit was therefore decreased and a region around the blade passing frequency excitation of the first natural frequency of the tower excluded. This led already to significant load reduction in fore-aft and sideways excitation, as shown in figure 3.2-2 and figure 3.2-3.

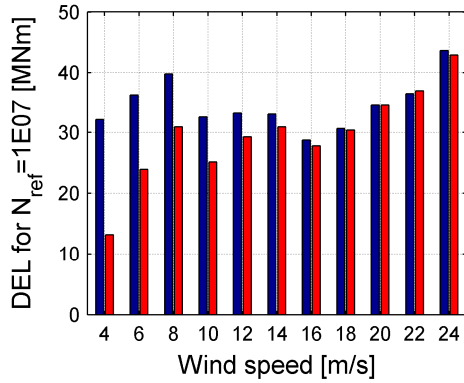


Figure 3.2-2: Comparison of old (blue) and new (red) reference control for sideways DELs at tower base

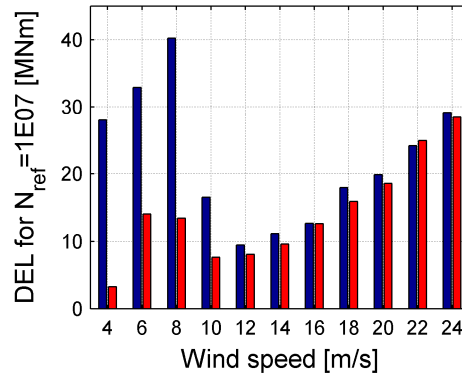


Figure 3.2-3: Comparison of old (blue) and new (red) reference control for fore-aft DELs at tower base

As can clearly be seen, the DELs in partial load region are still significantly higher than expected and seen for comparable wind turbines. This can mainly be explained by the broadband excitation around the natural frequency and is shown in a power spectral density plot in figure 3.2-4, where two wind speeds in partial load and in full load range are compared to each other. Although the vibrational energy in the tower bottom fore-aft oscillation is in principal higher for larger wind speeds, the higher energy is found around the natural frequency of the tower and support structure for the simulation with the lower wind speed of 8 m/s.

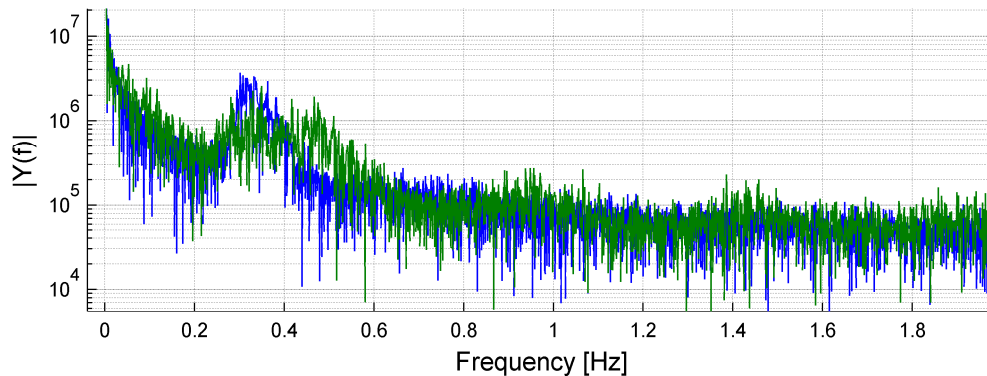


Figure 3.2-4: FFT of the tower base bending moment in fore-aft direction of a simulation of 8 m/s (blue) and 16 m/s (green) wind speed.

Several concepts for the mitigation of these resulting loads were introduced in deliverable D4.11. [ForWind-OL02]. They can be divided into control action based methods and structural control and damping concepts. In this report, the second option is discussed. Talking about a smart structure, one assumes to see an adjustable, reactive configuration of the support structure. Different concepts are under consideration regarding flexibility and adjustability of the support structure. However, to consider the structure really as being “smart” presuppose active and/or reactive elements to be integrated into the support structure. This would however be a second step. In the following, a first step is shown, which is still limited to passive devices to estimate optimal configurations and set values.

One of those concepts are vibrational load reduction systems located near the top of the wind turbine, see figure 3.2-5. Their advantage is omni-directionality and their optimal application is supposed to be where the accelerations are highest. This is where the effect is expected to be largest.

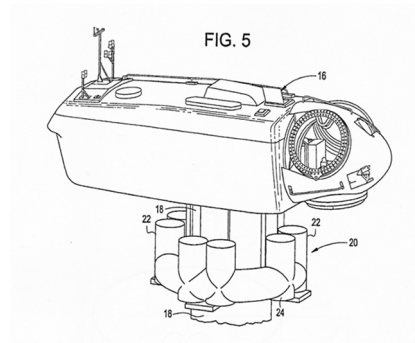


Figure 3.2-5: Vibration load reduction system located near a top of a tower of the wind turbine [ForWind-OL03]

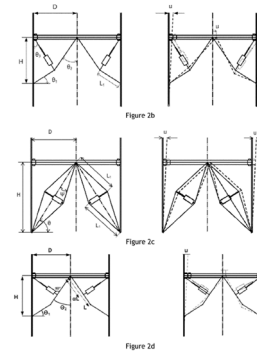


Figure 3.2-6: Displacement amplification configurations for viscous dampers [ForWind-OL04]

Another publication was released by Lackner et al [ForWind-OL05], describing the effect of passive structural control on wind turbines. The damper weight in this example is around 20 tons. The normal power production simulations with an optimal tuned mass damper at the nacelle proved a reduction of 4.5% in the tower fore-aft DEL when compared with the baseline. However, the side-to-side damage equivalent loads are increased by 1.4%.

Furthermore, also different positions for dissipation of vibrational energy in general can be thought of. Several concepts have therefore already been under investigation, such as the integration of torsional dampers at the transition piece [ForWind-OL01] or the integration of viscous dampers in brace configuration in the tower section. Figure 3.2-6 illustrates exemplary a vibration load reduction system, introduced by [ForWind-OL04]. It is based on the dissipation of lateral displacements of tower sections under use of viscous damper devices.

In the first part of the section 3.2.b. “Design results”, outcomes are presented for tuned mass dampers installed in the nacelle. Important parameters for these TMDs are the mass (absolute and in % of modal) and the tuning frequency. A parameter study was done under use of two tuning frequencies – 0.28 Hz and 0.3 Hz – and in total eight different mass ratios, ranging from about less than 900 kg to nearly 90 tons. Although the higher masses surely lead to substantial challenges in terms of integration and the increased overall tower top mass, they give a very good perspective of how load decrease is coupled to mass increase of the TMD. In the table 3.2-1, the values for the parameter study are listed.

Table 3.2-1: overview over damper mass, optimal damping for a tuned frequency of 0.3 Hz

modal mass	share of modal	mass of damper	mass of nacelle	optimal damping	tuned frequency	optimal damper frequency
[kg]	[-]	[kg]	[%]	[%]	[Hz]	[Hz]
862665	0.001	863	0.2	1.94	0.3	0.300
	0.005	4313	1.0	4.33	0.3	0.299
	0.01	8627	1.9	6.12	0.3	0.297
	0.025	21567	4.8	9.68	0.3	0.293
	0.05	43134	9.7	13.69	0.3	0.286
	0.075	64700	14.5	16.77	0.3	0.279
	0.1	86267	19.3	19.36	0.3	0.273
	0.125	107833	24.2	21.63	0.3	0.267

Table 3.2-1: overview over damper mass, optimal damping for a tuned frequency of 0.28 Hz

modal mass	mass of modal	mass damper	mass of nacelle	optimal damping	tuned frequency	optimal damper frequency
[kg]	[-]	[kg]	[%]	[%]	[Hz]	[Hz]
862665	0.001	863	0.2	1.94	0.28	0.280
	0.005	4313	1.0	4.33	0.28	0.279
	0.01	8627	1.9	6.12	0.28	0.277
	0.025	21567	4.8	9.68	0.28	0.273
	0.05	43134	9.7	13.69	0.28	0.267
	0.075	64700	14.5	16.77	0.28	0.260
	0.1	86267	19.3	19.36	0.28	0.255
	0.125	107833	24.2	21.63	0.28	0.249

The optimal parameter set for the tuned mass damper, the frequency and damping of the damper, respectively, is calculated according to [ForWind-OL06] with the following equations:

$$k_{opt} = \frac{1}{1+\mu} \quad (3.2-1)$$

where μ equals the mass ratio of the TMD mass to the kinetic equivalent structural mass.

and

$$k_{opt} = \frac{f_D}{f_{turbine}} \quad (3.2-2)$$

The necessary optimal damping coefficient can then be determined by

$$\zeta_{d,opt} = \sqrt{\frac{3\mu}{8 \cdot (1+\mu)^3}} \quad (3.2-3)$$

In the INN WIND.EU project, the evaluation and assessment of innovations is defined in deliverable D.1.12. “PI-based assessment of innovative concepts (methodology)” [ForWind-OL07], where a three stage approach is introduced. In this section, the first stage is partly evaluated for the integration of passive damping devices. The approach is defined in the style of IEC 61400-3 Ed. 1. [ForWind-OL08] – power production with normal turbulence and irregular waves with a JONSWAP Spectrum and idling with extreme wind model and 50 years significant wave height for extreme loads is to be considered. However, only fatigue loads are presented in the following and idling cases are, as wave excitation is in principle negligible for the overall fatigue loads, as shown in [ForWind-OL01], also omitted.

Regarding turbulence intensities and wave heights and periods, the design basis of UpWind.eu and the IEC standard with type class Ib was considered.

3.2.b Design results

The following graphs present the results for simulations including a passive tuned mass damper at tower top, installed in the nacelle. The damage equivalent loads are compared for IEC 61400-3 Ed.1 [ForWind-OL08] conformal simulations for wind speeds ranging from cut-in – 4 m/s – to cut-out wind speed – 24 m/s. The resulting DELs are calculated per time series for an estimated lifetime of 20 years and a number of reference cycles of 1E07. A lifetime weighted DEL is afterwards calculated, assuming Rayleigh distributed wind speed for an average wind speed of 10 m/s. However, for simplifications, no wind direction distribution is assumed.

Figure 3.2-7 shows the DELs at the tower base for the whole wind speed range in fore-aft direction. As can clearly be seen, the damper is most effective for wind speeds of 6 and 8 m/s in the overturning direction. The application of passive dampers might even lead to an increase in DEL, as seen for the 4 m/s wind speed bin. The tuning of the damper has therefore to be done very carefully.

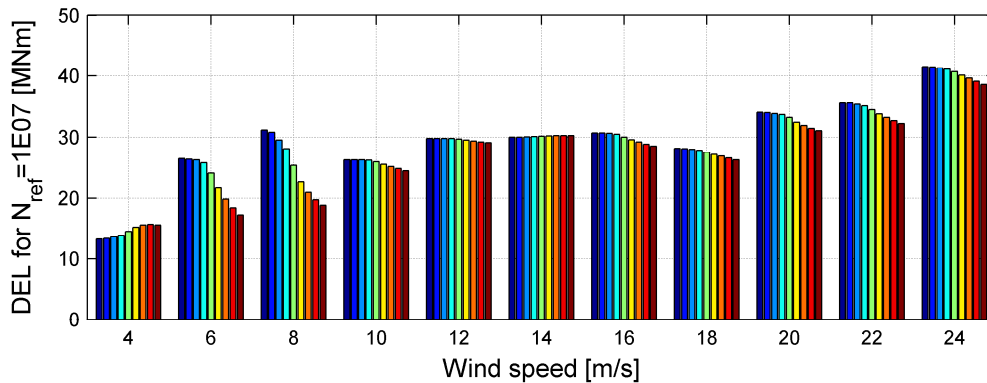


Figure 3.2-7: DELs at tower base in fore-aft direction with integrated dampers, reference in dark blue, additional bars according to the damper mass ratio as in table 3.2-1, tuned frequency 0.3 Hz

Figure 3.2-8 shows the results of the same simulations in sideways direction. Large load reductions can be found for all damper mass ratios.

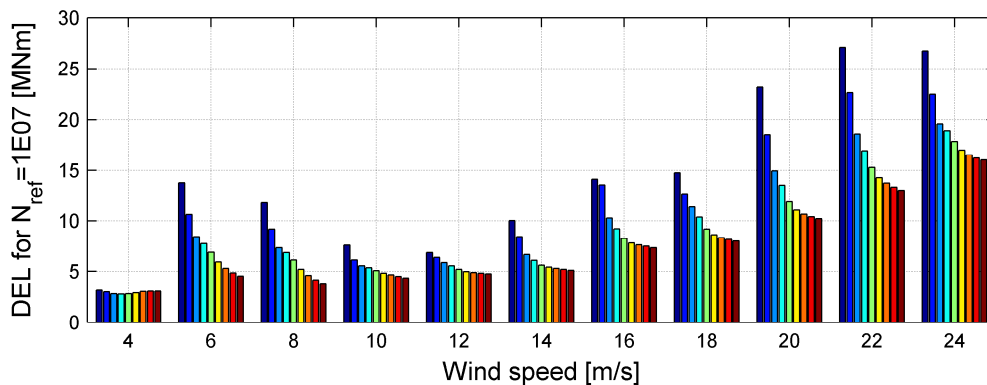


Figure 3.2-8: DELs at tower base in sideways direction with integrated dampers, reference in dark blue, additional bars according to the damper mass ratio as in table 3.2-1, tuned frequency 0.3 Hz

Load reduction at transition piece are desirable, however, the lowest support structure legs are the most critical parts in the design of the jacket. Whether the load mitigation is also transferred into the jacket and the lower legs is shown in the following. Therefore, two different wind and wave directions were investigated as indicated in figure 3.2-9.

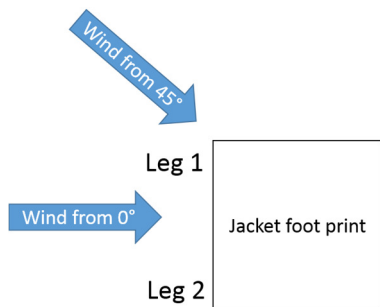


Figure 3.2-9: Scheme of Wind directions

Figure 3.2-10 shows the fatigue damage of the forces along the lower support structure leg member. The results are comparable to the results of the damage equivalent moment in overturning direction at the tower bottom. This leads to the conclusion, that the load mitigation not only affects the tower bottom, but also the lower leg parts of the jacket, where critical loads already occurred in the design phase and which are the design driving parts.

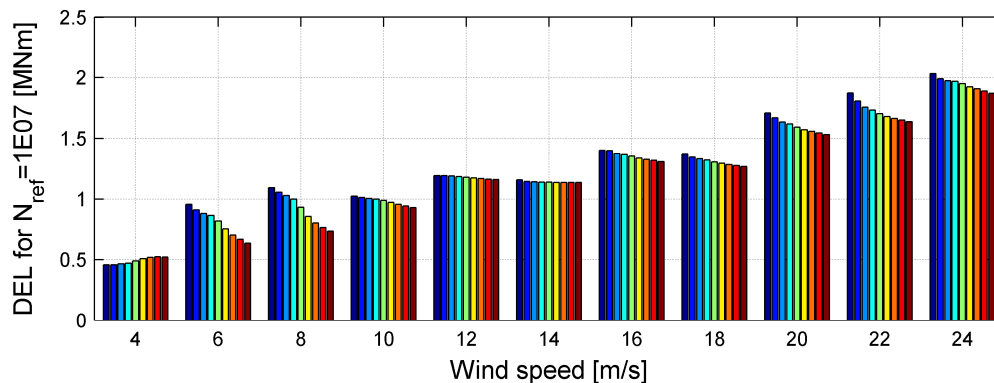


Figure 3.2-10: DELs at tower base in sideways direction with integrated dampers, reference in dark blue, additional bars according to the damper mass ratio as in table 3.2-1, tuned frequency 0.3 Hz

Table 3.2-3 summarizes the simulations by showing the relative lifetime weighted fatigue damage – compared between reference and applied damper – for different damper mass ratios, as described in table 3.2-1. Although higher mass ratios will result in enormous challenges regarding the integration, increased tower top mass and many more, already realistic masses up to 22 tons (mass ration of 0.025) lead to significant fatigue load reductions. Decreases ranging from nearly 4% for the fore-aft direction to over 40% in the sideways direction and also decreases of 5.68 to 7.26 for the support structure bottom legs can be realised. As expected, the most significant effect is seen for load directions, where least initial damping is present, namely the sideways direction and its lack of aerodynamic damping.

In addition, the analysis of the lower legs shows, that the load mitigation is indeed transferred also to the lower sections of the jacket. Two different wind direction were chosen as shown in figure 3.2-9. However, only the reference case and a damper mass ratio of 0.025 were simulated so far. The results show also large reduction in the analyzed fatigue forces along the member. It is however very remarkably, that the reductions are significantly higher if one leg is oriented in wind direction.

Table 3.2-3: Relative weighted life time DELs for a damper tuned for 0.3 Hz

Mass Ratio	0.001	0.005	0.01	0.025	0.05	0.075	0.1	0.125
Fore-aft in [%]	-0.25	-1.00	-1.92	-3.96	-6.09	-7.51	-8.70	-9.72
Sideways in [%]	-16.63	-30.88	-35.94	-41.64	-45.22	-47.11	-48.38	-49.35
Leg 1 for 0° in [%]	-2.62	-4.79	-5.75	-7.26	-8.61	-9.48	-10.19	-10.76
Leg 2 for 0° in [%]	-1.97	-3.47	-4.29	-5.68	-7.02	-7.95	-8.76	-9.51
Leg 1 for 45° in [%]				-17.56				
Leg 2 for 45° in [%]				-26.07				

As the load reduction might be very sensitive to variations of the tuning frequency of the mass damper, another configuration with a frequency of 0.28 Hz was also investigated.

The results are found in the following figures 3.2-11 and 3.2-12, and table 3.2-4. However, it can clearly be seen that the overall results in fatigue load reduction differ not significantly from the results for the damper, which was exactly tuned on the natural frequency of the system. One can conclude therefore, that the effect in load reductions is not very sensitive for alterations in the frequency in the investigated bandwidth.

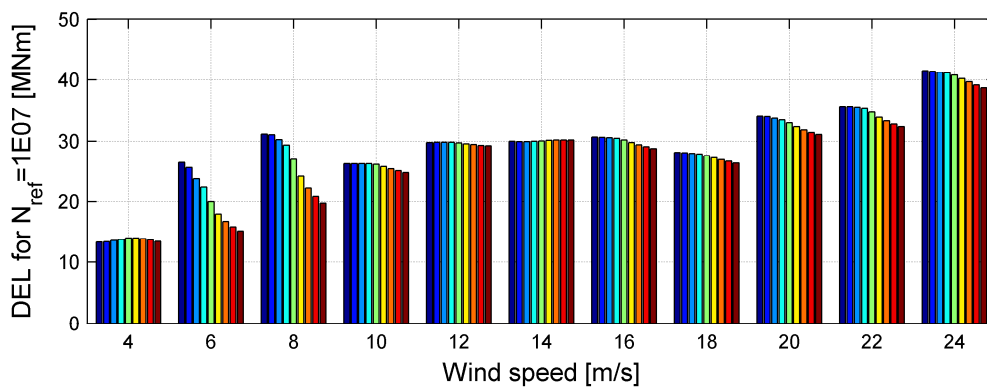


Figure 3.2-11: DELs at tower base in fore-aft direction with integrated dampers, reference in dark blue, additional bars according to the damper mass ratio as in table 3.2-1, tuned frequency 0.28 Hz

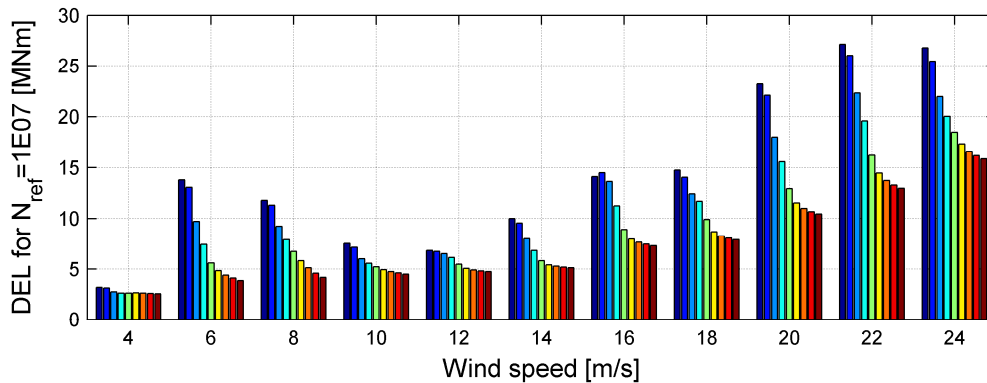


Figure 3.2-12: DELs at tower base in sideways direction with integrated dampers, reference in dark blue, additional bars according to the damper mass ratio as in table 3.2-1, tuned frequency 0.28 Hz

Table 3.2-4: Relative weighted life time DELs for a damper tuned for 0.28 Hz

Mass Ratio	0.001	0.005	0.01	0.025	0.05	0.075	0.1	0.125
Fore-aft in [%]	-0.32	-1.26	-2.12	-3.97	-6.01	-7.44	-8.56	-9.49
Sideways in [%]	-4.18	-18.36	-28.26	-38.64	-44.27	-46.87	-48.43	-49.58

The effect of the mass damper is, as expected, also seen in the spectrum of the tower base moment sideways signal. Figure 3.2-13 shows a comparison between the reference case (blue) and the applied damper with a mass ratio of 0.025 (green) for a wind speed of 8 m/s. The main blade passing frequency bandwidth can be seen for both signals, whereas the excitation of the natural frequency of the tower, shown as sharp peak at 0.3 Hz, is only seen for the reference case without damper. Its appearance in the signal is nearly completely mitigated by the tower damper.

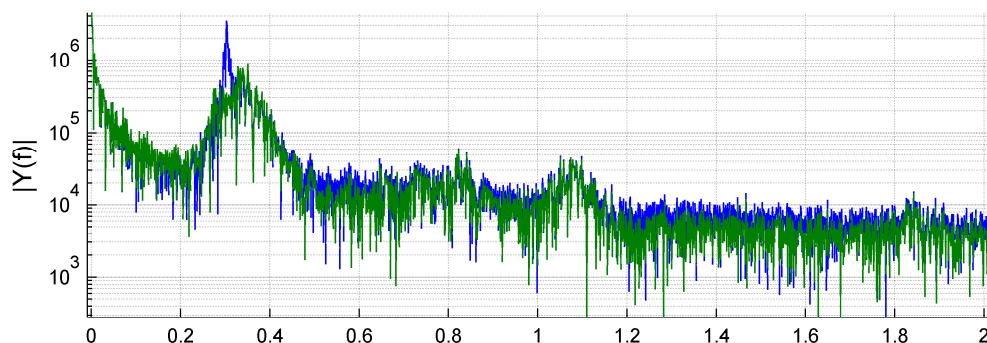


Figure 3.2-13: FFT of the tower base sideways moment of a simulation with 8 m/s wind speed, reference (blue) and tuned damper at 0.3 Hz with mass ratio of 0.025 (green)

3.2.c Conceptual conclusions and outlook

As described in the earlier section, significant load reductions at tower bottom as well as in the support structure legs can be achieved by implementation of tuned mass dampers in the nacelle with a reasonable mass ratio. These reductions are mainly driven by the mitigation of the resonance with the first natural frequency of the tower system. One could also consider the option to tune the dampers for different natural frequencies of the system.

The next steps to be taken are a more in-depth validation of the simulation results also for the braces, with more variation in the tuning frequency of the damper and with more wind directions. Also idling simulations should then be taken into account to evaluate the concept against the reference for the full operational range. The different tuning frequencies might then provide different optimal frequencies over the operational range, which might then lead to the necessity to tune the dampers while operation.

Furthermore, as seen in the FFT in figure 3.2-13, the damper only mitigates loading at a certain frequency. Viscous dampers, which dissipate in principle energy over the whole spectrum, might reduce the oscillations over a broader frequency range and therefore lead to further load reductions. Their application will be assessed in the future project work.

The evaluation was done under use of the 10 MW INN WIND.EU reference turbine. As already shown in the preceding figures, the energy, which is captured by the rotor out of the wind and the blade passing wide bandwidth excitation lead to a relatively high fatigue level. The effect of additional damping is in these cases proven to have significant influence and large potential for load reductions. For the next step in the project, from 10 MW to 20 MW wind turbines, this effect will even more increase. The rotational speed is again lower than for the 10 MW reference turbine and will more coincide with the natural frequencies of the system. The large rotor area and rated power introduces a large amount of energy into the system. The potential for load mitigation strategies, especially structural control and damping, is therefore considered to be very high.

References

- [ForWind-OL01] INN WIND.EU Deliverable D4.12., “Innovations on component level”, 2014
- [ForWind-OL02] INN WIND.EU Deliverable D4.11., “State of the art on component level”, 2013
- [ForWind-OL03] Zheng, D., Pierce, K. G., Ali, M. & Kothnur, V, “Vibration load reduction system for a wind turbine”, Patent, EP1677003 A2, 2006.
- [ForWind-OL04] Tsouroukdissian, A.R., “System and method for damping vibrations in a wind turbine”, Patent, EP2295795 A1, 2011.
- [ForWind-OL05] Lackner, M. A., Rotea, M. A., “Passive structural control of offshore wind turbines”, *Wind Energy*, Vol.14, pp. 373–388, 2011.
- [ForWind-OL06] Maurer & Söhne, „Tuned mass and viscous dampers“, 2004.
- [ForWind-OL07] Innwind.EU - Deliverable 1.21, „Reference Wind Turbine Design“, 2013
- [ForWind-OL08] IEC 61400-3 International Standard, „Wind Turbines – Part 3: Design requirements for Offshore Wind Turbines“, First Edition, 2009.

3.3 Hybrid jacket

3.3.a Introduction

Sandwich tubes for offshore support structures

The whole mass and therefore the costs of an offshore support structure depend on the water depth which it has been designed for. In the general case, where the structure consists only of steel pipe members, it can be assumed that the whole mass increases approximately quadratically with water depth. One promising possibility to cut the material costs, especially for big structures, is the usage of hybrid members in multi-member support structures like jackets. Hybrid members or so called sandwich tubes usually have a non-metallic core, which might be an elastomer, grout or concrete, enwrapped with steel faces at the inner and outer diameter (Figure 01). Due to the considerably better buckling behaviour of sandwich tubes compared to steel tubes [LHU01] it seems possible to reduce the structural mass and therefore the overall costs for offshore wind energy in this way. But there are many issues that have to be solved before an application of sandwich tubes in offshore structures is possible.

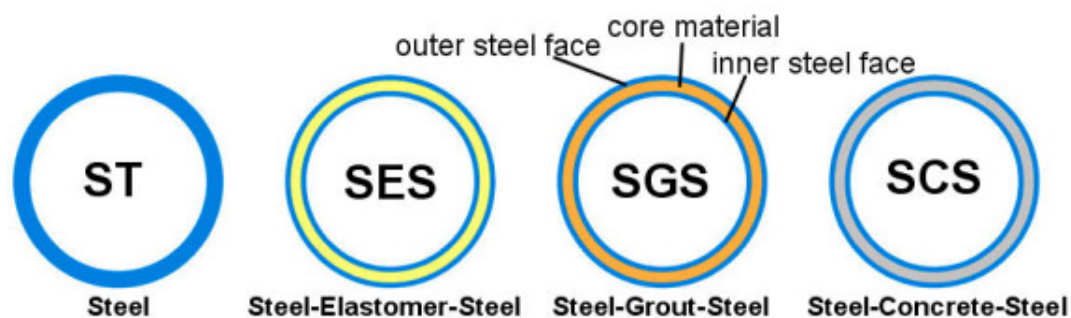


Figure 3.3-1: Various shell types, according to Schaumann & Keindorf [LHU01]

Challenges and solution strategies using hybrid members in a bottom-mounted jacket

An offshore structure has to withstand many kinds of loads and for this reason there is a comprehensive design process that consists mainly of three parts:

- Natural frequency analysis (NFA)
- Ultimate load state (ULS)
- Fatigue load state (FLS)

All these points are part of the certification process of an offshore support structure. For a large and heavy substructure the ultimate load state might be problematic due to high gravitational and inertial loads. This leads to shell buckling in case of too small pipe thicknesses. According to Schaumann and Keindorf [LHU01], [LHU02] and Schaumann et al. [LHU03] the usage of appropriate core materials can increase the shell stability and therefore the ultimate limit state loads. For example, a 25 mm steel / 30 mm grout / 25 mm steel sandwich element (inner steel face thickness / core thickness / outer steel face thickness) has a 27% greater buckling resistance than a steel tube with 50mm thickness, but is just

17% heavier (for a pipe section with a length of 30m and a diameter of 5.5m). This effect can be enhanced by the use of high-strength steels. Hence there is a capability to reduce the tube mass for constant buckling resistance.

The fatigue behaviour of shell tube joints is still objective of research and also main part of the upcoming experiments in work package 4.1. The weak points in steel structures are usually the welds between steel tubes and joints. It is also a great challenge to construct the connections between sandwich tubes in a way that the overall structure lifetime is not decreased. Some realization possibilities are discussed in deliverable D4.1.1 [LHU04]. However, this has to be investigated in detailed experiments.

The computational analysis of a hybrid jacket will lead to issues due to non-linear material behaviour, which has to be considered for structural finite element analyses as well as for the determination of ultimate load states. For example a shell with concrete as core material will withstand high uniaxial compressive loads, but just low tensile or flexural loads. Hence it has to be analysed at which locations it might be possible to replace a steel member with an appropriate hybrid member and where not. Moreover it has to be considered that the overall structure bending eigen frequencies (1st side-side and 1st fore-aft) lie in the “allowed range” between first and third order of the rotor rotating excitation frequency.

Another important factor is the cost aspect. One has to take into account that the manufacturing process of a sandwich tube is much more expensive than a pure steel tube and weigh the odds against the costs.

Design approach for bottom-mounted hybrid-jacket

Base for the design of the bottom-mounted hybrid-jacket is the reference jacket design which is a X-braced, four-legged state of the art design that has already been reported in deliverable D4.3.1 [LHU05] and in the design basis [LHU06].

In the first design step, the reference jacket is remodelled in ANSYS. The main challenge in this step is to reproduce the modal behaviour of the whole system in order to get sufficient simulation results especially with regard to the natural frequency analysis and model verification.

In the next step some quantities are defined to characterise sandwich sections with as few parameters as possible. Then a natural frequency analysis will be performed to ensure that the first structural bending eigen frequencies lie in the range between first and third order of the rotor rotating excitation frequency for several hybrid jacket types. For this purpose, it is sufficient to linearize the nonlinear material behaviour.

The third design step contains an analysis of the reference structure with regard to the design loads to find potential members that might be replaced by sandwich tubes. Sandwich tubes are expected to have a better buckling behaviour than pure tubes. There have not yet been made experiences with hybrid members for jackets, but experiments are scheduled for end of year 2014 in work package 4.1 to quantify the fatigue and buckling behaviour of various material combinations. The experimental results will build the foundation for a preliminary design of the hybrid-structure. A transient simulation of the preliminary hybrid structure with the design load cases DLC 1.1, 1.2 and 6.1 (according to deliverable D1.2.3) will be performed. Since it is expected that the overall mass and therefore the inertia and dead loads can be reduced by the usage of sandwich tubes, it has to be analysed whether it is possible to reduce the diameter or wall thicknesses of the pure steel members in the jacket. Of course,

the first bending eigen frequencies always have to be regarded. All transient calculations will be performed with the open-source aero-hydro-servo-elastic simulation code FAST, which has an integrated FEA-solver for the representation of multi-member bottom-fixed substructures in the module SubDyn. There have to be made some changes in FAST code, for example to consider the soil-pile behaviour or to output stresses, too.

Step four includes a comprehensive verification of the hybrid jacket design considering eigen frequencies, ultimate and fatigue limit states and a stage 3 (full assessment) proof according to deliverable D1.2.3, which implies all relevant design load cases. One has to distinguish between pure steel and hybrid members here: While conservative methods of load calculation are appropriate for steel tubes, they will not be applicable to sandwich tubes at all, so a parallel evidence process has to be made. The final point is then short a mass reduction study.

Figure 3.3-2 shows the four phases of hybrid-jacket design. Since the results of the experiments in work package 4.1 have not yet been finished are required for phase 3 and 4, this report handles particularly phase 1 and 2 of the design process.

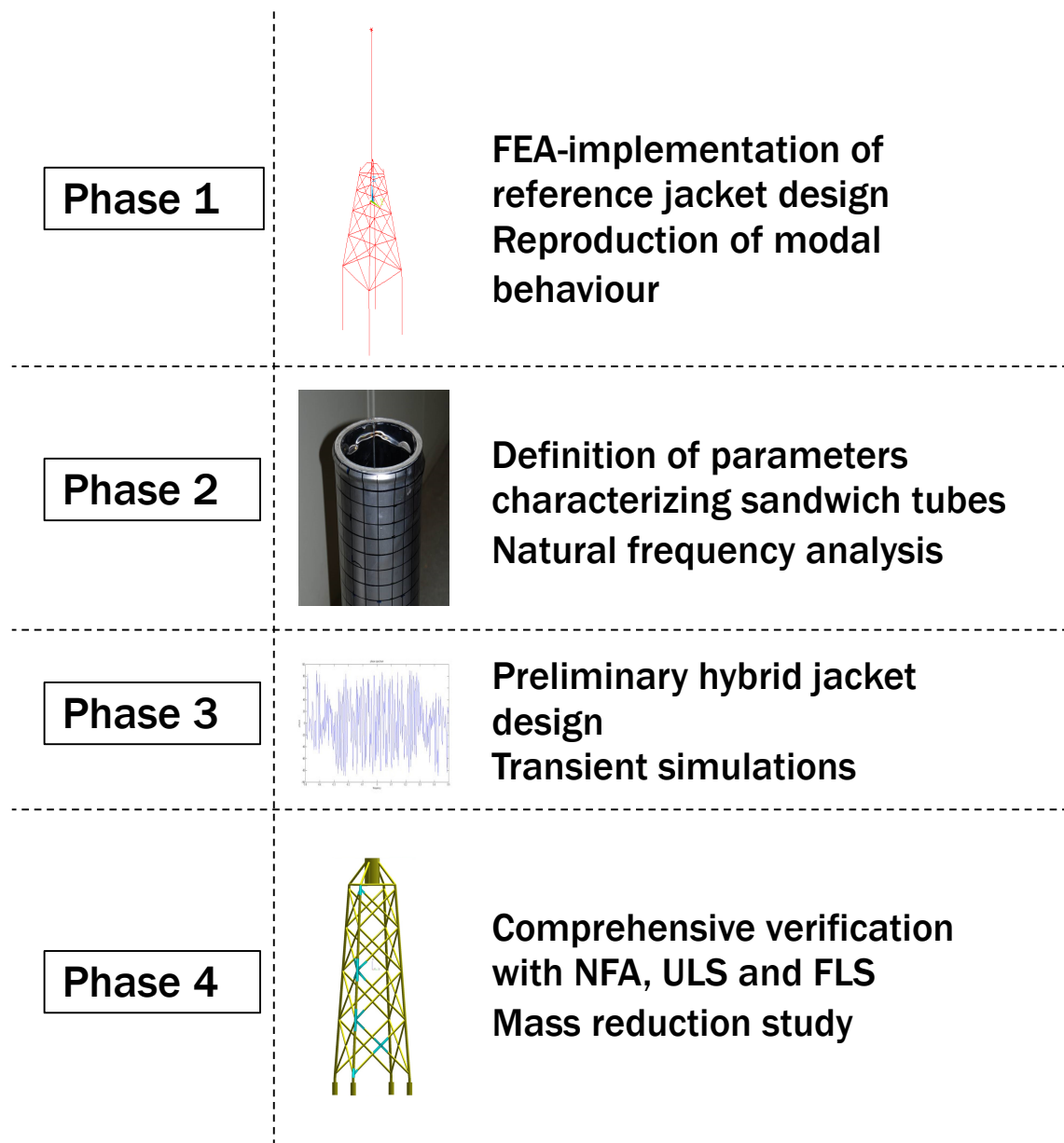


Figure 3.3-2: The four phases of hybrid-jacket design

3.3.b Design process

Phase 1: Implementation of reference jacket

The reference jacket design for the INN WIND.EU 10MW turbine is documented in the deliverable D4.3.1 [LHU05] and in the corresponding design basis [LHU06]. It is designed for a water depth of 50 meters and has 4 legs that are connected by four layers of X-braces. The design lifetime is 25 years and it has been modelled with the Ramboll in-house FEA-application ROSAP.

Especially for natural frequency analysis the reference jacket has been transferred to an ANSYS model (Figure 3.3-3) where the structure is discretised with 2-node-Timoschenko beam elements (beam188). The rotor-nacelle-assembly is treated as a mass point on tower top with discrete mass and inertia tensor taking into account the inertia of a distributed continuous rotor, soil-pile-interaction is considered by non-linear spring elements with specified force-deflection curves along the piles. Moreover the effects of corrosion, marine growth and added masses within flooded elements as well as outside the structure can be considered if desirable (for natural frequency analysis, fatigue conditions are presumed). The effect of joint flexibility is neglected here, since it has been experienced that it does not impact the eigen frequencies too much.

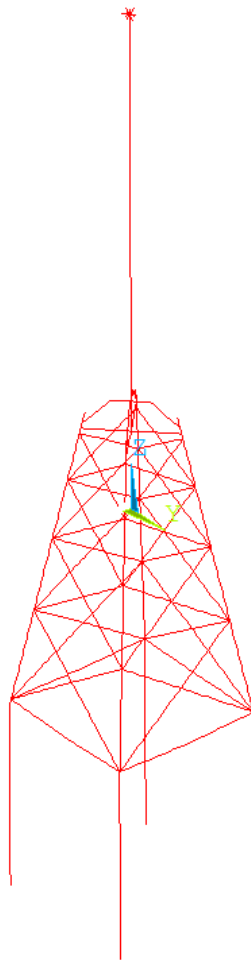


Figure 3.3-3: ANSYS FE-beam model of reference jacket

The differences in implementation and code mannerisms lead to the issue that a transfer to another FEA-solver might lead to slightly varying structural eigen frequencies. Table 3.3-1 shows that the accordance of the first two bending and torsional eigen frequencies are very good, but there is a slight difference of about 10% between the calculated values for the second bending modes. The reason might be that secondary structures have been neglected in the ANSYS model. This has to be considered for the interpretation of results.

Table 3.3-1: Calculated eigen frequencies (in Hz) for the total reference jacket structure including tower and tower-top-mass with ROSAP and ANSYS (considering fatigue conditions)

	1 st side-side	1 st fore-aft	1 st torsional	2 nd side-side	2 nd fore-aft
ROSAP	0.2867	0.2885	0.9358	1.1003	1.1133
ANSYS	0.2924	0.2944	0.9223	1.2031	1.2296
Difference	+2,0%	+2,0%	-1,4%	+9,3%	+10,4%

Phase 2: Definition of properties characterising sandwich tubes and natural frequency analysis

Phase 2 consists mainly of 2 steps: The first one is a definition of conceivable hybrid elements depending on representative parameters. In the second step it has to be analysed whether the critical structural eigen frequencies are impacted by the usage of hybrid members or not.

For reasons of simplification it is assumed that the fictive sandwich materials can be described by varying values of tube thicknesses (the outer diameters remain constant compared to the reference jacket, see Figure 3.3-4 for all occurring quantities) and densities and have linear-isotropic material behaviour (with steel properties). In this case, one can define a mean density of the sandwich tube $\bar{\rho}_{Sandwich}$:

$$\bar{\rho}_{Sandwich} = \frac{\rho_{Core} \cdot (r_3^2 - r_2^2) + \rho_{Facing} \cdot (r_4^2 - r_3^2 + r_2^2 - r_1^2)}{r_4^2 - r_1^2}$$

To characterize several variants of sandwich elements two auxiliary measures and one boundary condition are defined (since there are three thicknesses, three equations are necessary to describe a sandwich element). The factor c_1 is defined as the proportion of the core thickness to the thickness of the corresponding thickness of the reference jacket steel tube t_{ref} :

$$c_1 = \frac{r_3 - r_2}{t_{ref}}$$

The factor c_2 defines the proportion of the sandwich tube thickness to the reference jacket steel tube thickness:

$$c_2 = \frac{r_4 - r_1}{t_{ref}}$$

Obviously for $c_1 = 0$ and $c_2 = 1$ one gets the steel reference jacket. Moreover it is assumed that the thicknesses of inner and outer facings are identical:

$$r_2 - r_1 = r_4 - r_3$$

For a preliminary study on hybrid jackets, it is presumed that either all leg pipes or all brace pipes between the joints are replaced by sandwich elements (elements related to the joints are neglected here because only sandwich members are regarded). While the experimental investigations on hybrid elements have not been done so far, various combinations of parameters $\bar{\rho}_{sandwich}$, c_1 and c_2 shall be analysed neglecting the fact that the outcome from the numerical study might be not applicable to real applications (in fact, this section just handles the impact of sandwich elements on modal properties of the whole structure).

According to the experiences with sandwich tubes in literature [LHU01], [LHU02], [LHU03] it is reasonable to vary the parameter c_1 in a range from 0,2 to 0,4 and the parameter c_2 in a range from 0,8 to 1,2. Of course, this leads to a reduction of required steel mass, but it cannot be expected that this correlates to a cost reduction due to the sophisticated production process of sandwich pipes.

Regarding the reference jacket design report it is obvious that the circumferential welds between the brace pipes are exposed to lower fatigue loads than those between the leg elements and the joint welds. Requirement for further use of the results of this study is that there is no significant worse fatigue behaviour of sandwich elements and their connections to other elements compared to pure steel elements.

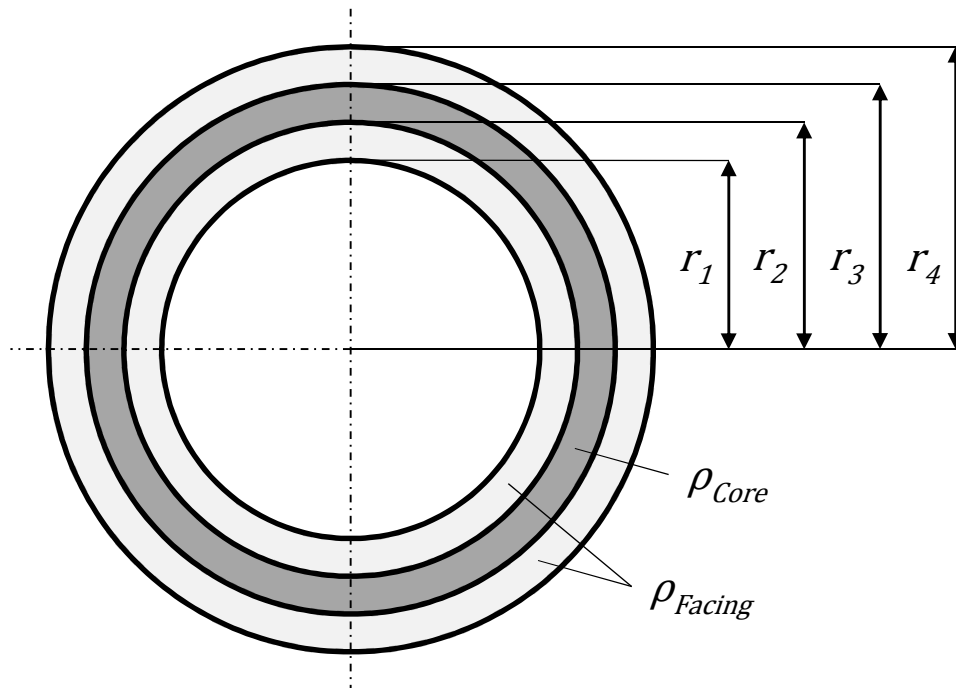


Figure 3.3-4: Cross-section of sandwich tube with corresponding quantities

Table 3.3-2 shows the calculated eigen frequencies in dependency of the parameters c_1 and c_2 . A core density of $\rho_{core} = 2300 \frac{kg}{m^3}$ (concrete or grout) has been presumed for all analyses.

One obtains very low changes in the global eigen frequencies in each case, especially for the critical first two bending eigen frequencies. Hence there is no risk to leave the allowable frequency range with regard to the rotor excitation frequency, even for a “worst case scenario”, where the jacket consists of many sandwich elements. Comparing the first and second bending mode shapes of a representative hybrid jacket approach (Figure 3.3-5) with those from the reference jacket [LHU07], there are no remarkable differences, too. In fact, not every parameter set would be applicable, especially for those elements with high utilization ratios of ULS loads.

One can conclude from this study that even for the simplifications that have been made there will be no significant impact on the natural frequencies or the corresponding mode shapes. So the next step is to obtain a preliminary hybrid jacket design for the INN WIND.EU – 10 MW turbine.

Table 3.3-2: Calculated eigen frequencies (in Hz) for the total hybrid jacket structure including tower and tower-top-mass (considering fatigue conditions), relative change of hybrid jacket eigen frequencies compared to correspondent steel structure eigen frequencies in brackets

	1 st side-side	1 st fore-aft	1 st torsional	2 nd side-side	2 nd fore-aft
Sandwich braces, steel legs	0.2924 (+0.0%)	0.2944 (+0.0%)	0.9223 (+0.0%)	1.2074 (+0,4%)	1.2349 (+0,4%)
$c_1 = 0,2$ $c_2 = 1,0$					
Sandwich braces, steel legs	0.2924 (+0.0%)	0.2944 (+0.0%)	0.9223 (+0.0%)	1.2096 (+0.5%)	1.2375 (+0.6%)
$c_1 = 0,3$ $c_2 = 1,0$					
Sandwich braces, steel legs	0.2924 (+0.0%)	0.2944 (+0.0%)	0.9224 (+0.0%)	1.2117 (+0.7%)	1.2401 (+0.9%)
$c_1 = 0,4$ $c_2 = 1,0$					
Sandwich braces, steel legs	0.2923 (+0.0%)	0.2943 (+0.0%)	0.9162 (-0.7%)	1.2045 (+0.1%)	1.2313 (+0.1%)
$c_1 = 0,3$ $c_2 = 0,8$					
Sandwich braces, steel legs	0.2925 (+0.0%)	0.2945 (+0.0%)	0.9264 (+0.4%)	1.2115 (+0.7%)	1.2399 (+0.8%)
$c_1 = 0,3$ $c_2 = 1,2$					
Steel braces, sandwich legs	0.2924 (+0.0%)	0.2944 (+0.0%)	0.9224 (+0.0%)	1.2070 (+0.3%)	1.2343 (+0.4%)
$c_1 = 0,2$ $c_2 = 1,0$					
Steel braces, sandwich legs	0.2924 (+0.0%)	0.2944 (+0.0%)	0.9224 (+0.0%)	1.2090 (+0.5%)	1.2366 (+0.6%)
$c_1 = 0,3$ $c_2 = 1,0$					
Steel braces, sandwich legs	0.2924 (+0.0%)	0.2944 (+0.0%)	0.9224 (+0.0%)	1.2110 (+0.7%)	1.2390 (+0.8%)
$c_1 = 0,4$ $c_2 = 1,0$					
Steel braces, sandwich legs	0.2889 (-1.2%)	0.2909 (-1.2%)	0.9222 (+0.0%)	1.1974 (-0.5%)	1.2259 (-0.3%)
$c_1 = 0,3$ $c_2 = 0,8$					
Steel braces, sandwich legs	0.2948 (+0.8%)	0.2968 (+0.8%)	0.9225 (+0.0%)	1.2162 (+1.1%)	1.2431 (+1.1%)
$c_1 = 0,3$ $c_2 = 1,2$					

According to the higher fatigue loads at the welds between the leg pipes it might be advisable to concentrate on the brace pipes for further investigations on hybrid jackets. Particularly the second and third layers of X-braces are exposed to relatively low fatigue and high buckling

loads. However, this is part of phase 3 & 4 in the hybrid jacket development, thus it will be explored in the subsequent deliverable.

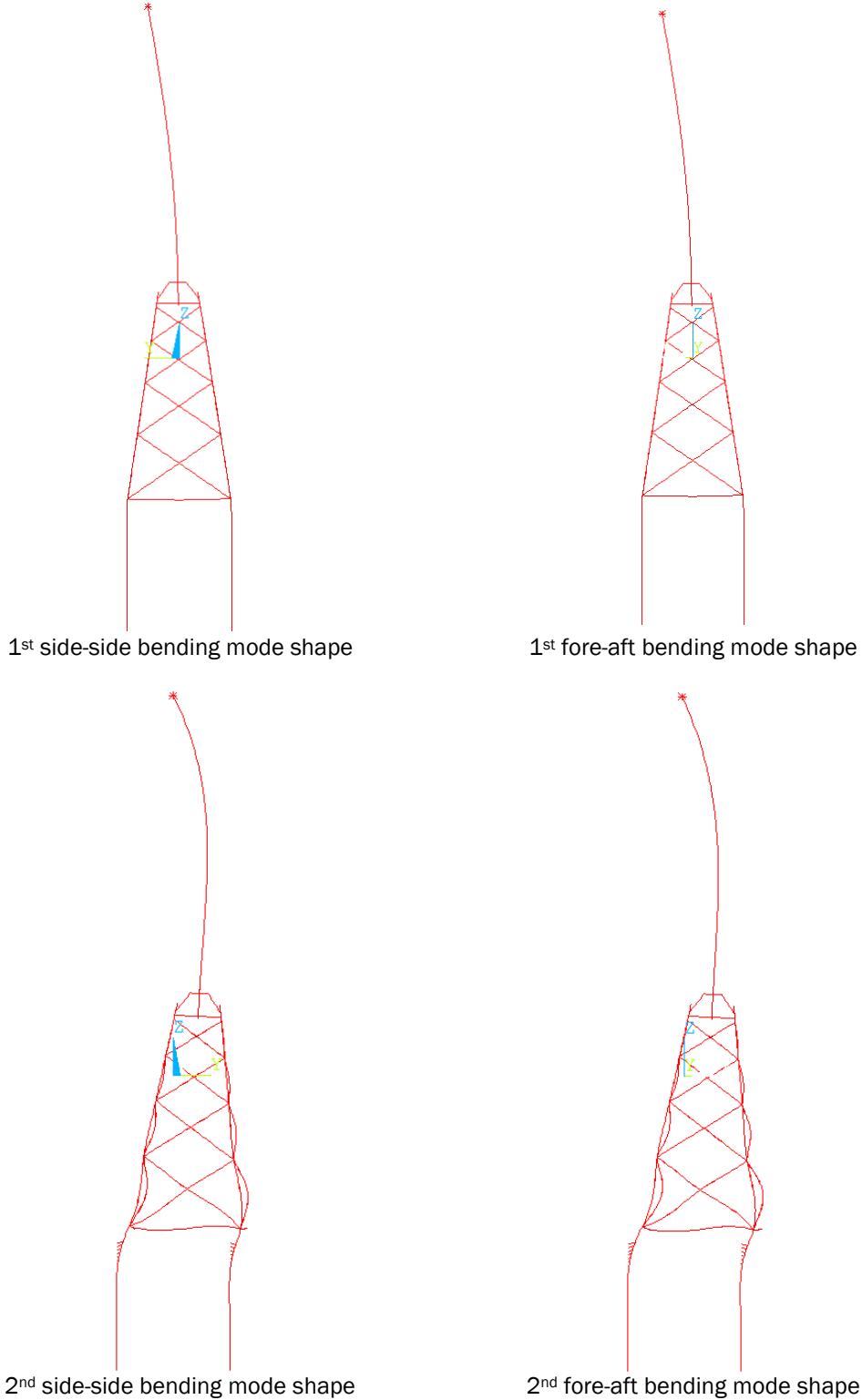


Figure 3.3-5: Bending mode shapes of hybrid jacket with steel braces and sandwich legs
 ($c_1 = 0.3, c_2 = 1.2$)

3.3.c Conclusion and Outlook

Sandwich tubes offer the possibility to produce jacket elements with much better buckling behaviour compared to pure steel tubes, which has been shown in several publications and which lead to the idea to use them in support structures for high water depths, where the buckling loads are higher than in more shallow water. Nevertheless, there are some challenges prohibiting a broadband application at the latest state of the art. The common design methods for bottom-mounted steel support structures rely mainly on natural frequency analysis, fatigue and ultimate limit state. For hybrid jackets these methods have to be adjusted and some simplifications have to be made to allow preliminary studies on these innovative offshore substructures.

In this report some assumptions about the material behavior have been required to perform a numerical natural frequency analysis of a preliminary hybrid jacket and it has been shown that for reasonable parameters the resulting eigen frequencies as well as the corresponding mode shapes do not differ very much from those of the reference jacket. This is an important point for the design of a hybrid jacket, since there is no risk to hit the “forbidden” frequency range of rotor excitation. However, there are several open questions, especially regarding the buckling and fatigue behaviour of sandwich elements and not least the unknown production costs. These are the upcoming tasks of the hybrid jacket development and they will depend very much on the experiments in work package 4.1. Most likely, it cannot be expected that a hybrid jacket will contribute to cost reduction very much at this state of the art, as long as the production costs of sandwich elements exceed the costs of steel pipes supposedly by far. Moreover sandwich elements are not appropriate to address the main problem of the reference jacket, namely the insufficient lifetime of joint welds, particularly the K-joints at the brace-to-leg connections. However, the outcome from this study should be a contribution to the development of innovative composite materials for offshore support structures.

References

- [LUH01] Boggs, P. T., & Tolle, J. W., “Sequential Quadratic Programming. *Acta Numerica*”, 1995
- [LUH02] Borstel, T. v., “INN WIND.EU Deliverable 4.3.1 Design Report Reference Jacket”, INN WIND.EU, 2013
- [LUH03] Conn, A. R., Scheinberg, K., & Vicente, L. N., “*Introduction to Derivative-Free Optimization*”, SIAM, 2008
- [LUH04] DNV., “DNV-RP C203: 2012-10 DNV Recommended Practice – Fatigue Design of Offshore Steel Constructions”, DNV, 2012.
- [LUH05] “INN WIND.EU – 10MW Jacket Interface Document for Preliminary Jacket Design”, INN WIND.EU, 2013.
- [LUH06] “INN WIND.EU Deliverable 1.2.1 Definition of Reference Wind Turbine”, INN WIND.EU, 2013.

3.4 Jacket-Bucket-Concept

3.4.a Introduction

Objective of this document

The purpose of this document is to evaluate today's state-of-the-art design approaches for suction bucket foundations and to compare the suction bucket solution with the pile solution as a supporting member of the Reference Jacket in terms of weight and costs. Furthermore, already installed suction bucket projects are presented and potential uncertainties regarding the design of suction buckets are summarized. Finally, further need of research is identified which is required to reduce the conservatism inherent in today's design procedures of suction buckets.

The Suction Bucket Principle

Suction buckets consist of a cylindrical welded steel structure open at the bottom and a stiffened lid at the top which transfers the loads from the upper structure to the circumference of the bucket. Buckets can either be used as mono-bucket foundations or as multi footing structures similar to a common tripod or jacket with piles replaced by buckets, see Figure 3.4-1. Penetration into the seabed is achieved by applying suction inside the caisson. The generated hydrostatic pressure difference results in an additional driving force. Furthermore, the tip resistance is reduced when installed in sand due to induced seepage flow around the lower edge. Consequently, no heavy installation equipment is required apart from pumps. In contrast to the common piling process required for pile installation, noise emission is not an issue when installing suction buckets. In general, suction buckets are assumed to offer a high potential of decreasing the cost of energy.

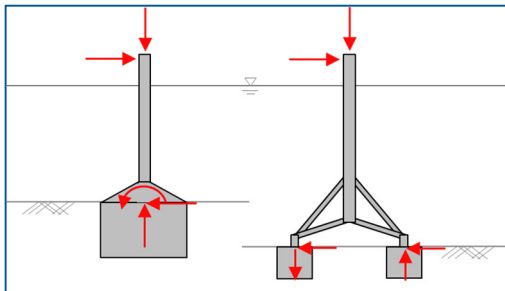


Figure 3.4-1: Suction Buckets as a Mono-Bucket (left) and a Multi-footing (right) Foundation.

Moreover, suction buckets can be removed by reversing the installation process and may be reused at another location. The suction anchor concept has been used in the oil and gas industry since the early 1980s. However, the dynamic loading characteristic acting on offshore wind turbines differs significantly from the predominantly static loading characteristic of oil and gas structures. Consequently, the experience from the oil and gas industry can hardly be transferred.

The suction bucket foundation can be floated and taken to the installation site by tug boats. Alternatively, they can be installed ship-based. In any case no heavy installation equipment is required and no offshore lifting crane is needed if suction buckets are floated. The Offshore Standard DNV-OS-J101 [RAMBOLL02] regards suction buckets as “well suited for sites with water depth ranging from 20 to 50 metres”. Nielsen [RAMBOLL01] expects the bucket to be the lighter and more cost-effective solution compared to piled foundations. In some cases the

foundation can already be connected to the superstructure during fabrication. With respect to the limiting installation criteria the weather window can be increased compared to piling procedures since the suction bucket installation is less sensitive in terms of the maximum allowable significant wave height. No seabed preparation is required and an integral scour protection is possible [RAMBOLLO1].

On the other hand the fabrication of suction buckets is known to be more complex compared to the fabrication of piles. Moreover, a jacket with buckets is expected to require more space than similar structure with piles because of the larger bucket surface which is required in order to achieve the same bearing capacity [RAMBOLLO3]. One third of the designed prototypes have failed which underlines the uncertainties dominating the design and installation process of suction buckets [RAMBOLLO4].

Obviously, the suction bucket concept offers the opportunity to offset some of the piled foundation's disadvantages. However, the lack of standardized design procedures for both the installation process and the load-bearing behaviour has led to rather conservative design approaches. Consequently, more detailed investigations are required in order to establish less conservative design methods considering for example beneficial effects from suction during rapid tensile loading and therefore more cost effective designs.

Examples of Installed Suction Bucket Foundations

In order to provide an overview of suction bucket foundations already installed, information about completed projects have been collected and summarized in Figure 3.4-2. This list of foundations and full-scale prototypes is intended to provide an overview rather than a complete summary. The only known suction bucket foundation which actually supports an offshore wind turbine is the one to be installed in August 2014 as part of the *Borkum Riffgrund* Wind Farm. In addition, there have been three successfully installed suction buckets which support met-masts (*Horns Rev II*, *Dogger Bank*) and some more intended to support platforms. Furthermore, two prototype projects have been carried out (*Wilhelmshaven*, *Frederikshavn*).

			Diameter [m]	Height [m]	Water depth [m]	Structure	Successfully Installed
Foundations							
HORNS REV II	2009	Met-mast	12	6	15	Mono	✓
FIRTH OF FORTH	2012		15	12		Mono	?
DOGGER BANK	2013	Met-mast	15	7.5	~23	Mono	(✓)
KEPPEL VEROLME	2013	Substation	11	9.5	40	Tetra	✓
AMSTEL	2013	Platform	7.4	7	20	Tetra	✓
WINTERSHALL'S L6/B	2014	Platform	10	9		Tri	✓
BORKUM RIFFGRUND	2014	Turbine	10	9		Tri	
Prototypes							
WILHELMSHAVEN	2005	Turbine	16	15	4	Mono	No
FREDERIKSHAVN	2002	Turbine	12	6	4	Mono	✓

Figure 3.4-2: Examples of Installed Suction Bucket Foundations.

3.4.b Design of Suction Buckets for the Reference Jacket

3.4.b.1 General

The design process illustrated in Figure 3.4-3 represents the rather conservative state-of-the-art approach. The red boxes highlight the analyses that are carried out as part of this study. Based on initial dimensions of the buckets the required suction for installation is determined and compared to the critical suction with regard to both hydraulic failure and buckling of the shell structure. The resulting bucket dimensions provide the basis for the bearing capacity calculations including tensile and compressive loading as well as overturning moment. Within a full design the empty box at the bottom should be filled with the SLS/FLS design. However, these were not taken into account at this stage of the study. Any effects of cyclic loading have been neglected.

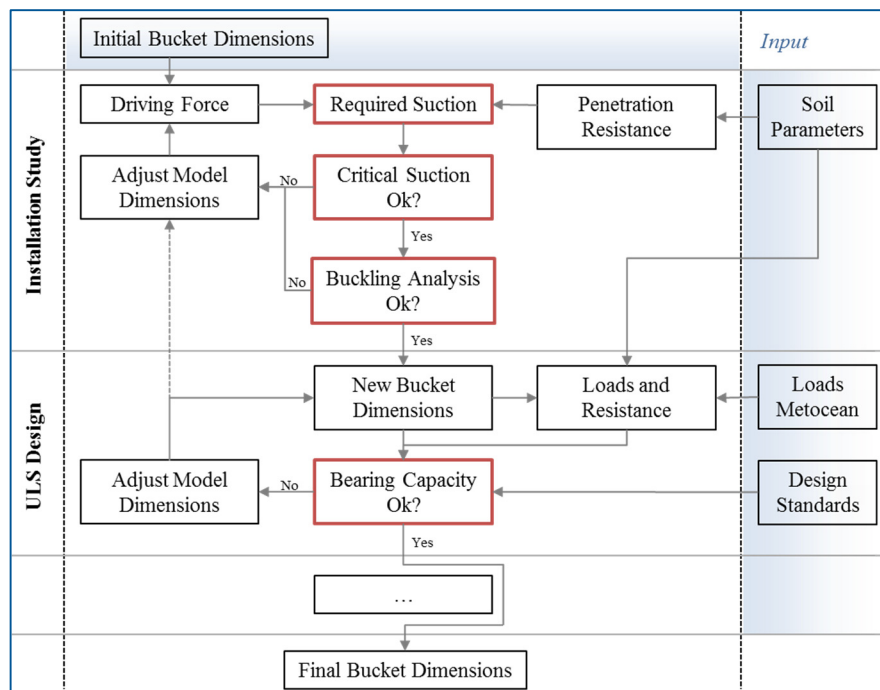


Figure 3.4-3: Overview of the design process scheme.

3.4.b.2 Design Input

Bucket Dimensions

The dimensions of the suction buckets are given by a diameter of $D = 10$ m, a skirt length of $h_b = 13$ m and a skirt wall thickness of $t = 30$ mm. An overview of the considered bucket system is displayed in Figure 3.4-4. Please note that all diagrams given in the following sections refer to this geometry, at least with regard to the diameter and the wall thickness of the skirt.

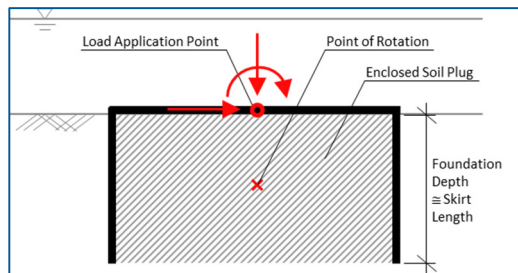


Figure 3.4-4: Simplified system of the bucket.

Loads

The maximum design loads can be seen in Table 3.4-1. The loads have been extracted at mudline level from the analysis of the reference jacket with piles, ref. [RAMBOLLO6], and safety factors are already included.

Table 3.4-1: Design Loads derived from the Reference Jacket Design, ref. [RAMBOLLO6].

	Fz [MN]	Fxy [MN]	Mxy [MNm]
Max. Tension	16.2	5.2	8.3
Max. Compression	-27.8	6.4	11.6

Soil

The relevant soil parameters are taken from the soil profile provided for the Reference Jacket, ref. [RAMBOLLO6]. The permeability of the soil is assumed to be 0.0001 m/s. As the soil inside the bucket is possibly loosened due to seepage, an increased inner permeability of approximately 0.0003 m/s may describe the actual conditions more accurately.

3.4.b.3 Installation Process

General

The installation of suction buckets is possible in both sand (relatively high permeability) and silt or clay (low permeability). The benefit gained from the applied suction depends on the soil parameters. The installation process can be divided into two phases: During the initial phase the bucket penetrates the seabed due to the effective self-weight of the structure. This can be increased by additional ballasting. No suction is applied at this early stage as it would lead to erosion of the seabed. It is recommended to achieve sufficient self-penetration depth in order to avoid hydraulic failure in the next phases. Several practical cases show that around 1 m of initial penetration is sufficient [RAMBOLLO5].

Subsequently, the pressure inside the sealed bucket is slowly lowered while pumping out the water. The pumping rate is increased until it reaches a defined level, but always smaller than the critical suction, at which hydraulic failure is likely to occur. During the second phase - the suction assisted phase - the increased pumping rate is kept constant until the final depth is reached. The applied suction leads to an additional vertical force induced by the hydrostatic pressure difference over the lid of the caisson. In granular soils the applied suction generates a water flow around the tip of the skirt and thus reduces the effective stresses. Accordingly, the tip resistance is reduced and the caisson continues penetration.

The limiting critical suction is defined by the hydraulic gradient which reduces the effective stresses down to zero and liquefaction potentially occurs in case of sand while a clay layer is more exposed to plug lift-up. Analytical approaches for calculating the critical suction are included in this analysis.

Required Suction

In general the self-weight penetration depth occurring during the first phase is calculated by skin friction and tip resistance on the one hand and the sum of submerged weight and additional ballasting on the other hand. By solving the equilibrium of forces the unknown penetration depth h can be determined.

For the second phase the equilibrium of forces is extended by the applied suction and can again be solved for the penetration depth h . The way of considering the applied suction during installation in sand differs from one approach to another. While some approaches consider a modified unit weight of the soil and consequently a change of skin friction, others account for a reduction of the end bearing.

The installation approaches used in this study were taken from DNV [RAMBOLL07], Senders and Randolph [RAMBOLL09] and Houlsby and Byrne [RAMBOLL08]. The DNV approach is originally intended for skirted foundations. Thus, no suction is taken into account. DNV provides parameters within the equation to define a “highest expected” and a “most probable” value. Senders and Randolph extended the DNV approach by introducing a ratio describing the relation between the inner and outer permeability in order to take the installation effects into account. This way the analysis is adapted to the properties of suction buckets and considers the suction by an additional driving force as well as a reduction of inner skin friction and end bearing. The approach by Houlsby and Byrne is based on the effective stress in contrast to the other two approaches that are CPT-based. It considers increasing vertical stresses due to skin friction and the effect of suction on skin friction and end bearing using a modified pore pressure distribution. Figure 3.4-5 shows the required suction according to the above mentioned approaches.

Critical Suction due to Hydraulic Failure

In general the suction should never exceed the critical hydraulic gradient. Limitations are given by the risk of liquefaction (if the effective vertical stresses are reduced to zero by the hydraulic gradient) and cavitation (if pore water pressure decreases below the atmospheric pressure).

Approaches by Houlsby and Byrne [RAMBOLL08], Clausen and Tjelta [RAMBOLL11], Guttormsen [RAMBOLL12] and Feld [RAMBOLL13] are considered, whereat the ones according to Clausen and Tjelta [RAMBOLL11] and Feld [RAMBOLL13] are valid for an aspect

ratio of $h_b/D < 0.5$ only. Correspondingly the equations are valid for skirt length of up to 5m in the given case with a diameter of $D=10\text{m}$. The results are shown in Figure 3.4-5. The approaches appear to be in good agreement. However, the “highest expected” value of the DNV approach exceeds the critical suction. Since this value represents an upper bound it is expected to be non-critical for the design. From literature review and comparison to previous projects it can be assumed that the installation of the suction bucket with the given dimensions would be feasible under the given site conditions and that the “highest expected” value overestimates the resistance.

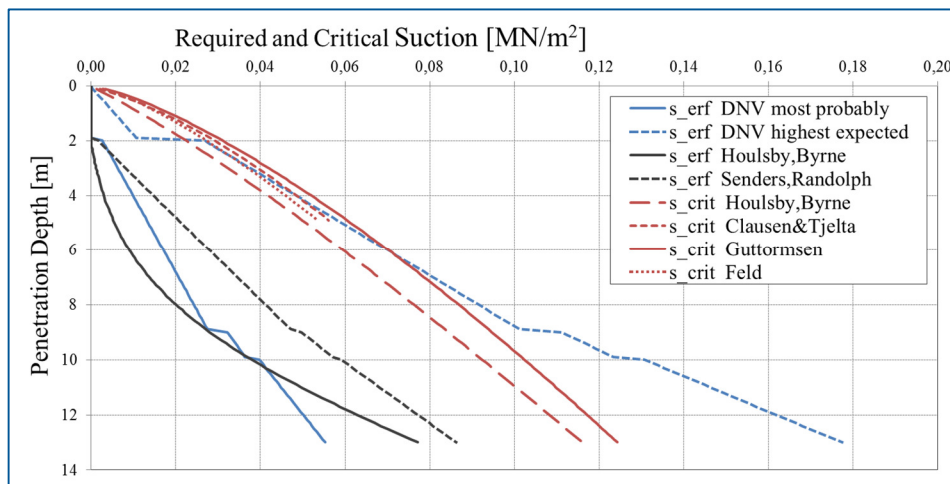


Figure 3.4-5: Required and critical suction depending on the penetration depth.

Critical Suction due to Buckling

The risk of buckling failure due to the applied suction inside the bucket is considered by approaches according to EC 3 [RAMBOLL17] and Pinna [RAMBOLL15]. The latter has been extended due to recommendations by Le Blanc [RAMBOLL16] in the form of the so called equivalent embedment depth. Therein the lateral restraint by the surrounding soil is taken into account, which is also applied to the EC3 approach within this report.

The boundary conditions are defined by a clamped support at the upper and a pinned support at the lower edge. The surrounding soil is assumed to support the shell structure. The bucket is assumed to be a single shell element. Welded connections are not considered. The results are displayed in Figure 3.4-6. Obviously the critical buckling pressure P_{cr} is higher than the one required for installation (compare Figure 3.4-5 with Figure 3.4-6). The approaches according to EC 3 [RAMBOLL17] and Pinna [RAMBOLL15] result in constant critical pressures, while the influence of the considered increasing lateral restraint with higher embedment depth is represented by the dashed lines.

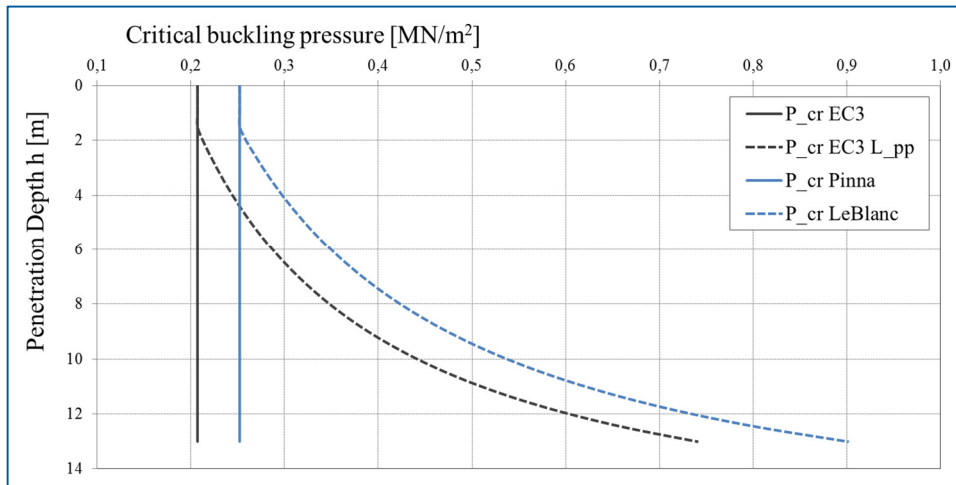


Figure 3.4-6: Critical buckling pressure depending on the penetration depth.

3.4.b.4 Ultimate Limit State

General

Due to the overturning moment induced by wind and waves, vertical forces are the dominating forces acting on buckets supporting jackets. In general, the resistance of buckets against these vertical forces is formed by the skirt's inner and outer wall friction as well as end bearing at the tip of the skirt. An additional capacity from the lid may be considered. The lid is - in case of compressive loading - comparable to a flat foundation element (with zero depth) in contact with the soil.

Since no specific bucket design approaches are available so far, classical pile design equations from API [RAMBOLL18] are adopted in combination with individual modifications. However, applicability of these equations remains limited since the dimensions are far out of the actual validity range. For the tensile capacity - apart from the outer wall friction - either the inner wall friction or the weight of the soil plug should be assessed, whichever is less. It is not clear to what extent an additional resistance generated by the low-pressure below the lid is assessable.

Ultimate Limit State

The ultimate compressive bearing capacity determined from different approaches can be seen in Figure 3.4-7. Pile design approaches according to API and DNV have been used as well as gravity base approaches according to API [RAMBOLL18], DNV [RAMBOLL02] and EC 7 [RAMBOLL19]. The pile design curves include an additional compressive bearing capacity created by the lid, roughly estimated by assuming a flat foundation element with zero embedment depth pushing against the soil.

Within the gravity base calculations the enclosed soil plug is assumed to be part of the foundation and the whole structure is treated as a rigid body. An internal failure is not considered. The load eccentricity and the resulting effective foundation area as well as the load inclination are based on the ULS loads given above and determined according to API [RAMBOLL18]. The assumptions made for the gravity base approach are expected to overestimate the capacity while those based on the pile design approach are assumed to be on the safe side. It is worth mentioning that, depending on the applied standard, different partial safety factors have been considered to derive the design compression capacity. When comparing the design compressive capacity with the maximum compressive design load given in Table 3.4-1, it becomes obvious that the compressive capacity is sufficient for the chosen geometry.

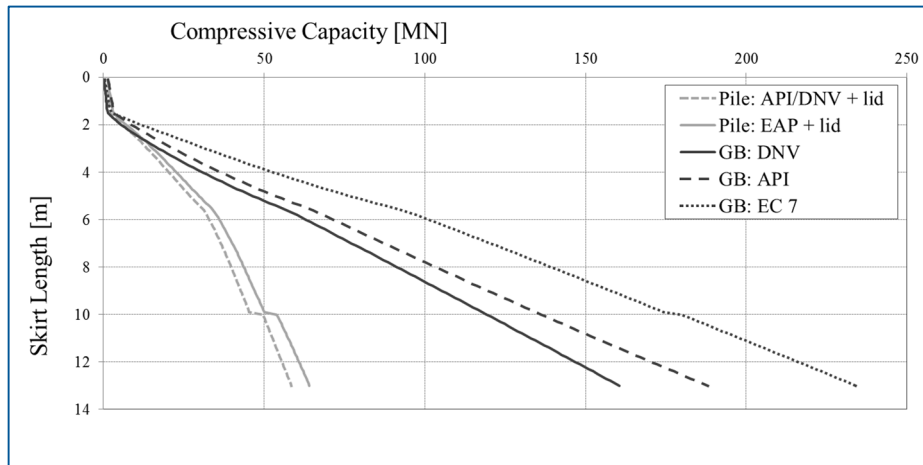


Figure 3.4-7: Design Compressive Capacity depending on the skirt length.

Figure 3.4-8 shows the lateral capacity according to DNV's pile design approach and the magnitude of passive earth pressure pushing against the outer skirt wall. The load application surface of the earth pressure is set to the length of the skirt times the height of the bucket, which is a conservative approximation. The DNV curves are determined by use of the p-y-method originally intended for slender piles. Since applicability is already limited for large diameter monopiles it is even more arguable for the applicability of suction buckets. Nonetheless, it provides an estimation of the lateral capacity. It should be noted that, depending on the applied standard, different partial safety factors have been considered to derive the design lateral capacity. When comparing the design lateral capacity with the maximum lateral design load given in Table 3.4-1, the lateral capacity shows sufficient resistance for the chosen geometry.

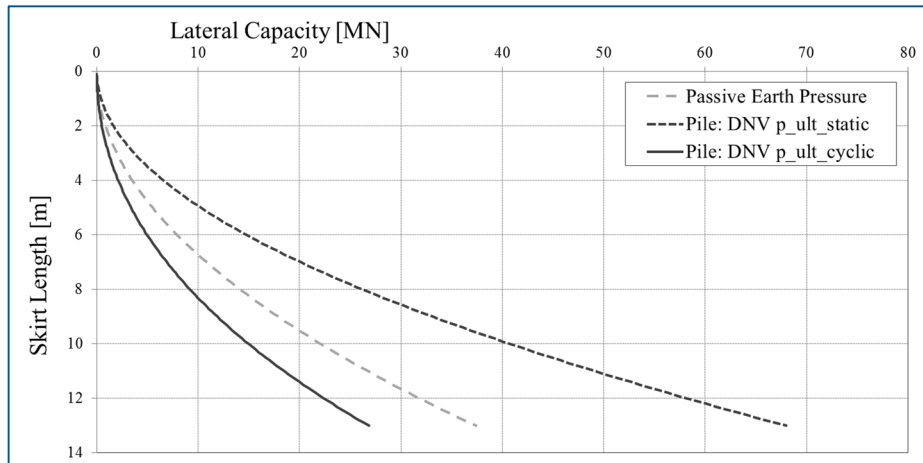


Figure 3.4-8: Design Lateral capacity depending on the skirt length.

Since no permeability of the soil is provided in [RAMBOLL06], it is assumed to be 0.0001 m/s which is a typical value for cohesionless soils in the North Sea. In order to account for an increase of permeability inside the bucket due to applied suction during installation, a lower and an upper bound is defined. For the lower value a permeability ratio of 1 is assumed while for the upper a ratio of 3 is expected. The realistic conditions are assumed to lie in between these two values. Figure 3.4-9 shows one curve for the approach according to Housby et al. [RAMBOLL10], one with the lower and one with the upper bound value. The impact of this value on the bearing capacity becomes obvious and underlines the need of further

investigations with regard to this topic. In addition, results derived from calculations according to Deng and Carter [RAMBOLL20] as well as API [RAMBOLL18] are shown.

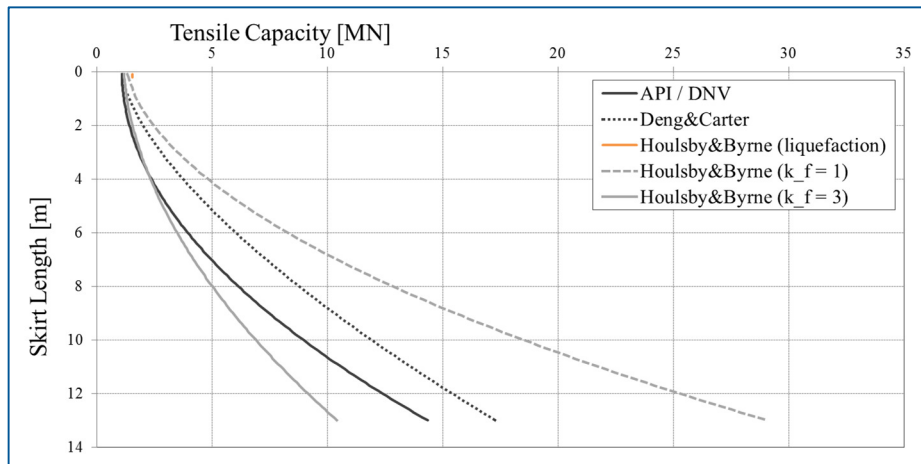


Figure 3.4-9: Design Tensile Capacity depending on the skirt length.

When comparing the design tensile capacity with the maximum tensile design load given in Table 3.4-1, it becomes obvious that for the chosen geometry the tensile capacity is sufficient according to the approach by Deng & Carter as well as according to Houlby & Byrne in case of a permeability ratio of 1. Contrarily the maximum tensile design load slightly exceeds the design tensile capacity according to the API/DNV approach as well as according to Houlby & Byrne when taking a permeability ratio of 3 into account. In this context it is worth mentioning that from recent investigations it has been found that an additional capacity originating from the suction inside the bucket under short-term rapid tensile loading can be expected. However, it is not quite clear yet how to calculate this beneficial resistance. As tension appears to be the decisive load case, certainty about the suction effect may have a great impact on the cost-effectiveness of suction buckets.

Considering the reserves inherent in the impact of this beneficial effect as well as the relatively large deviation of the approaches presented above, it can be concluded that the tensile capacity for the chosen geometry is sufficient to withstand the acting forces.

3.4.b.5 Other limit states to be considered

The mobilization of the full soil resistance is assumed to be activated at a certain settlement of the bucket. Since the serviceability of offshore wind turbines is strongly dependent on deformations – especially tilting – of the foundation, the design should include determination of the permanent and cyclic displacements. As approaches considering long-term cyclic behavior are rare, they should be conservatively estimated using results from laboratory tests in combination with the predicted short term displacements and rotations.

In case of jacket structures the differential settlement between the compression and the tension bucket would be most critical. It may be estimated by determination of the heave of the tension leg and the settlements of the compression leg. These calculations should consider immediate displacements after installation, those from consolidation after mounting of turbine and permanent displacements from accumulated shear deformations during cyclic loading.

A fatigue limit state analysis should consider the fatigue of the steel bucket which will typically feature several circumferential and longitudinal butt welds prone to fatigue. No fatigue analysis of the steel bucket has been conducted at this stage of the study.

A natural frequency analysis should consider the natural frequency of the overall structure including the tower and RNA in order to check whether the structure's natural frequency lies within the allowable 1P-3P frequency bandwidth defined by the turbine manufacturer. No natural frequency analysis has been conducted at this stage of the study.

Furthermore, it should be noted that only the bucket has been considered in this study. The bucket lid - which forms the transition from the jacket leg to the bucket - has not been taken into account in the course of this study.

3.4.c Conclusion and Outlook

In this document today's state-of-the-art design approaches for suction bucket foundations have been evaluated and applied as an alternative to piles as a supporting member for the InnWind Reference Jacket [RAMBOLL06].

A bucket design has been performed for the Reference Jacket as explained in section 3.4.b. The required suction has been calculated based on formulas provided by DNV [RAMBOLL07], Senders and Randolph [RAMBOLL09] and Housby and Byrne [RAMBOLL08]. For calculation of the critical suction with respect to hydraulic failure the approaches offered by Housby and Byrne [RAMBOLL08], Clausen and Tjltta [RAMBOLL11], Guttormsen [RAMBOLL12] and Feld [RAMBOLL13] have been used while the formulas provided by DNV [RAMBOLL14], EC 3 [RAMBOLL17] and Pinna [RAMBOLL15] have been evaluated to determine the critical suction with respect to buckling of the bucket.

The ultimate limit state analysis has been conducted considering pile design approaches according to API and DNV as well as gravity base approaches according to API [RAMBOLL18], DNV [RAMBOLL02] and EC 7 [RAMBOLL19] in order to determine the ultimate compressive load resistance. The ultimate tensional load resistance has been determined in accordance with Housby et al. [RAMBOLL10], Deng and Carter [RAMBOLL20] as well as API [RAMBOLL18]. DNV [RAMBOLL02] has been used in order to calculate the ultimate resistance against lateral loads. No serviceability limit state and fatigue limit state has been taken into account in the course of this design.

In order to compare the both solutions - namely piles and buckets - the masses and anticipated costs are summarised in Table 3.4-2. For the piles a lumped sum price of 1500 Euros/ton is assumed while a lumped sum price of 2500 Euros/ton is considered for the suction bucket.

Table 3.4-2 Comparison of pile vs. bucket solution for the Reference Jacket

Type	Dimensions			Mass [tons]	Fabrication Costs**) [Euros]
	Diameter [m]	Wall Thickness [mm]	Length [m]		
Pile	2.438	32-52	41.5	95	130000
Bucket*	10.000	30	13.0	145	362500

*) including bucket cylinder (96 tons) top plate (31 tons) and transition to pile (18 tons)

**) based on lumped sum prices derived from experience

Even though the fabrication costs for the suction bucket seem to be very high, it should be noted that considerable saving potential for the bucket's fabrication costs can be expected due to more refined and less conservative design approaches. Moreover, the installation costs for suction buckets are expected to be much smaller compared to the installation costs for piles.

References

- [RAMBOLL01] Nielsen, O. J., "The Universal Foundation", in: Proceedings of Universal Foundation's Technical Conference, Hamburg, 2014.
- [RAMBOLL02] "DNV-OS-J101: Offshore Standard - Design of Offshore Wind Turbine Structures", Det Norske Veritas, May 2014.
- [RAMBOLL03] Zaaijer, M. B., "Comparison of Monopile, Tripod, Suction Bucket and Gravity Base Design for a 6 MW Turbine", in: Proceedings of the Offshore Windenergy in Mediterranean and Other European Seas (OWEMES) Conference, Naples (Italy), 2003.
- [RAMBOLL04] LeBlanc, C., Ahle, K., Nielsen, S. A. & Ibsen, L. B., "The Monopod Bucket Foundation - Recent Experiences And Challenges Ahead", in: Proceedings of European Offshore Wind Conference and Exhibition, Stockholm (Sweden), 2009.
- [RAMBOLL05] Romp, R. H., "Installation-Effects of Suction Caissons in Non-Standard Soil Conditions", M.Sc.-Thesis, Delft University of Technology, 2013.
- [RAMBOLL06] von Borstel, T., "InnWind Reference Jacket, Deliverable 4.3.1", Ramboll, 2013.
- [RAMBOLL07] "DNV 30.4: Foundations Classification Note No. 30.4"
- [RAMBOLL08] Housby, G. T. & Byrne, B. W., "Design Procedures for Installation of Suction Caissons in Sand", OUEL Report No 2268/4: Calculation Procedures for Installation of Suction Caissons, 2005b.
- [RAMBOLL09] Senders, M. & Randolph, M. F., "CPT-Based Method for the Installation of Suction Caissons in Sand", in: Journal of Geotechnical and Geoenvironmental Engineering 135, 14-25, 2009.
- [RAMBOLL10] Housby, G. T., Kelly, R. B. & Byrne, B. W., "The Tensile Capacity of Scution Caissons in Sand Under Rapid Loading", OUEL Report No 2275/05: Research on Offshore Foundations - Papers at the Symposium on Frontiers in Offshore Geotechnics, Perth, 2005b.
- [RAMBOLL11] Clausen, C. J. F. & Tjelta, T. I., "Offshore Platforms Supported by Bucket Foundations", in: Proceedings of 15th IABSE, Copenhagen, 1996.

- [RAMBOLL12] Guttormsen, T. R., Eklund, T. & Sparrevik, P., "Installation and Retrieval of Suction Anchors", in: Mooring & Anchoring, 1997.
- [RAMBOLL13] Feld, T., "Suction Buckets, A New Innovative Foundation Concept, Applied to Offshore Wind Turbines", Diss, Aalborg University, 2001.
- [RAMBOLL14] DNV, "Recommended Practice "Buckling Strength of Shells" (DNV-RPC202)", 2013b.
- [RAMBOLL15] Pinna, R., Martin, C. M. & Ronalds, B. F., "Guidance for Design of Suction Caissons Against Buckling During Installation in Clay Soils", in: Proceedings of 11th International Offshore and Polar Engineering Conference, Stavanger, Norway, 2001.
- [RAMBOLL16] LeBlanc, C., Ibsen, L.B. & Liingaard, M., "Buckling of Large Diameter Bucket Foundations During Installation in Sand", in: Diss. LeBlanc 'Design of Offshore Wind Turbine Support Structures', Technical University of Denmark, 2009a.
- [RAMBOLL17] DIN-EN-1993-1-6, "Eurocode 3 - Design of Steel Structures - Part 1-6: Strength and Stability of Shell Structures", German Version EN 1993-1-6:2007 + AC:2009, 2010.
- [RAMBOLL18] API, "Geotechnical and Foundation Design Considerations – Recommended Practice", (RP 2GEO), 1. Ed, 2011.
- [RAMBOLL19] DIN-EN-1997-1, "Eurocode 7 - Geotechnical Design - Part 1: General Rules", German Version EN 1997-1:2004 + AC:2009, 2009.
- [RAMBOLL20] Deng, W. & Carter, J. P., "Vertical Pullout Behaviour of Suction Caissons", Research Report, Centre for Geotechnical Research, The University of Sydney, 1999.

4 CONCLUSIONS AND OUTLOOK

Four completely different concepts were presented by four different project partners. As the development status of the innovative concepts differs significantly, giving a common conclusion and outlook might be very challenging.

It could be concluded, however, that all partners presented the advantages of their concepts compared with the reference design. In all cases, mass or load reductions and the application of a new foundation concept or new materials were proven. However, also the level of details of the evaluations in the earlier sections differ significantly. Each concept might need more investigations to ensure comparability with the other concepts and the reference turbine in terms of costs, applicability, and time to market and to be further assessed within the scope of the project.

In addition, one partner did not succeed in finishing his contribution in time. This leads the author to the recommendation of updating this report with more detailed results by the partners being more in-line with the project scope and the 3 stage approach for innovation assessment, given in deliverable D1.23. Included in the update, also an outlook towards the upcoming 20MW reference turbine is desirable. Furthermore, an assessment of the technology readiness level of the different innovative concepts and recommendations for their future development shall then be given.